SET PROJECT

STRUCTURAL ANALYSIS OF A TROUGH MODULE STRUCTURE, IN OPERATION AND EMERGENCY

Luca Massidda

Table of Contents

Introduction

In this report a structural analysis of trough module for a Concentrated Solar Power plant is discussed.
The attention is focalized on the structure of the trough, consisting in a 12m long steel frame, supporting an absorber tube, parallel to the structure axis, and a system of glass mirrors that form a parabolic shape and reflect the sunrays on the absorber tube. The tube is placed in the focus of the parabola.
A section of the structure is shown in the following figure.

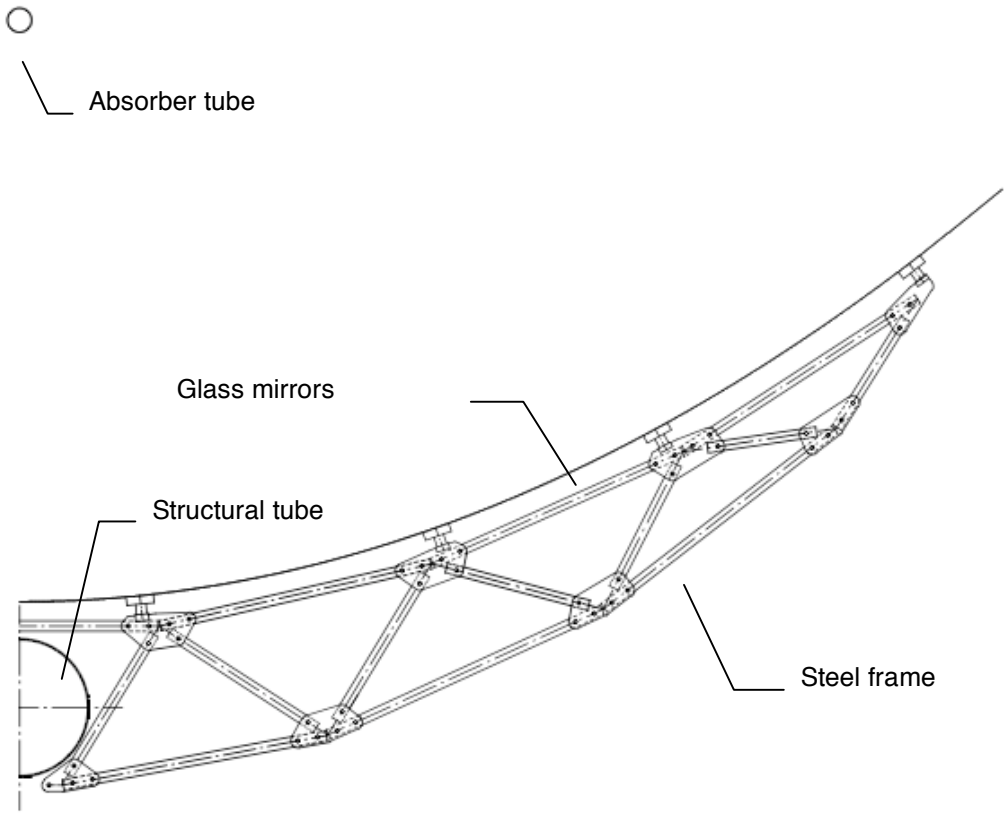

Figure 1 Section of the Trough structure

The structure is formed by a steel tube, to which are attached the absorber tube and the arms of the steel frame. This frame is connected to 28 glass mirror facets forming the reflective surface.
Both ends of the pipe are welded to support plates and through which several module are connected forming a line. A line may include 4 modules or more; the absorber tubes and the trough modules are welded to form a structure.
The line of through modules may rotate around an axis located near the center of gravity of the structure; this movement is due to an actuator system allowing the system to follow the sun position during the day.
The absorber tube is a compound tube formed by an internal stainless steel pipe, covered by a high absorbance and low emissive material, and protected by an external glass tube; a vacuum is produced between the steel and the glass. The absorber tube is connected to the structure with links that should keep the absorber tube on the focus of the parabola, and should allow the thermal expansions.
The numerical simulation of the structure is used to verify the strength of the system under the normal operating conditions and emergency conditions. Since the precision of the reflective surface is very important for the efficiency of the system a particular care has to be paid to the deformation calculation under operative conditions.

The loads acting on the structure are due to the self weight and to the action of the wind, since this structure may be assimilated to a wing connected to the ground. The required actuator torque will be evaluated as well.

Finite element analysis

Model description

A finite element model, representative of a possible structure has been created and analyzed by means of the ANSYS code.
The structure is not simple and a particular care has to be paid to the boundary conditions and to the connections between the different parts, since these details may have a remarkable effect on the results.
The structure may be divided in three parts:

- Mirrors
- Cantilever arms
- Structural tube

Mirrors

The reflective surface is composed by 28 mirrors (4 along the width and 7 on the length) each mirror is approximately 1.6m wide (arc length) and 1.7m long. The mirrors are made by glass and are 4mm thick.
Each mirror is supported in four points by the cantilever arms. The support point position is calculated in order to minimize the surface deformation in operating conditions; it can be shown that if we search for the distance between the symmetric support points in a uniformly loaded beam that gives the minimum angular deflection, this distance results to be proportional to the be a fraction of the beam length equal to 0.555. From this result we decided to put the distance between support points should be 0.555 of the mirror size in both directions.

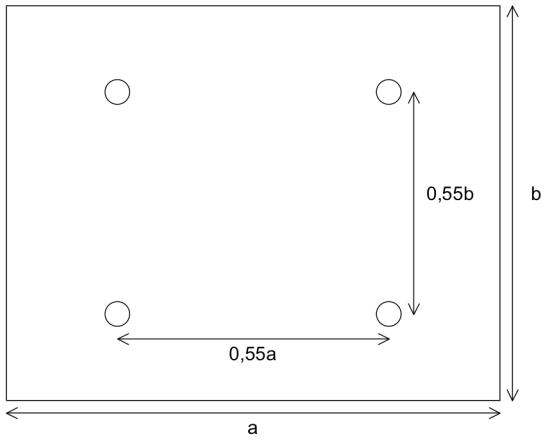

Figure 2 Mirror support points' position

Shell elements have been used to model these surfaces, specifically the SHELL63 element in ANSYS. Each mirror is modeled separately and has no continuity with the other mirror facets.

Cantilever arms

A truss of steel beams forms the cantilever arms. The beam section is constant along the truss, it is a hollow square section 30mm wide with a thickness of 2mm.
A beam element has been adopted for this portion of the structure, and ANSYS BEAM44 element has been used.

Tube

The structural tube is the main structural element of this design of the trough, all the loads acting on the structure are transferred to this tube, that acts as a simply supported beam for the wind pressure and self weight loads, and is also subject to the torque due to the wind action on the inclined parabolic profile.
The tube has an external diameter of 406.4mm and is 4mm thick, it's made from carbon steel.
This part of the structure is modeled using shell element and specifically the SHELL63 element in ANSYS.

Connections

As mentioned, the connection between the parts is important for the stress distribution and the deformation of the structure.
The ends of the model are rigidly inked to two nodes located in the rotation axis, in this way it has been avoided to include the detail of the support plates in the model. The boundary conditions of the supports are applied to these two additional nodes. The rotational axis is supposed to be on the axis of the parabola and 1.6m below the absorber tube.
The arms are linked to the structural tube with a rigid connection condition, which permits the rotation in the support points. The pipe sections where the arms are attached are forced to be rigid, this allows to emulate the behavior of the stiffening plates welded to the tubes and to which the cantilever arms should be attached.
Finally the mirrors are connected to the cantilever arms by modified beam elements with some rigidity components null. These elements allow simulating with accuracy the behavior of the actual supports. In this structure it is important that only (or mainly) the loads perpendicular to the mirror surface are transferred to the cantilever arms, and that no boundary is applied to the thermal expansion.

Material properties

The mechanical properties adopted for the steel structure and for the glass of the mirrors are reported in the following tables.

Table 1 Carbon steel mechanical properties

Density	7860	kg/m^3
Young' modulus	206	GPa
Poisson ratio	0,3	-
Thermal exp. coeff.	$12.0\ 10^{-6}$	K^{-1}
Yield stress	240	MPa
Allowable stress	160	MPa

Table 2 Glass mechanical properties

Density	2400	kg/m^3
Young' modulus	69	GPa
Poisson ratio	0.2	-
Thermal exp. coeff.	$8.0\ 10^{-6}$	K^{-1}
Rupture stress	30	MPa
Allowable stress	12	MPa

Boundary conditions

A single module of the trough is considered. The structure is supported at the two ends, and basically acts as a simply supported beam with a 12m span.
The support nodes are located at the two ends, along the rotation axis, that is parallel to the absorber tube and 1.6m below it.
These nodes are rigidly linked to the ends of the structural tube; these connections have the same function of the end plates in a real structure.
The displacements along the vertical (Y) and transverse (X) directions are blocked at both ends; axial (Z) displacements are blocked at one end only.

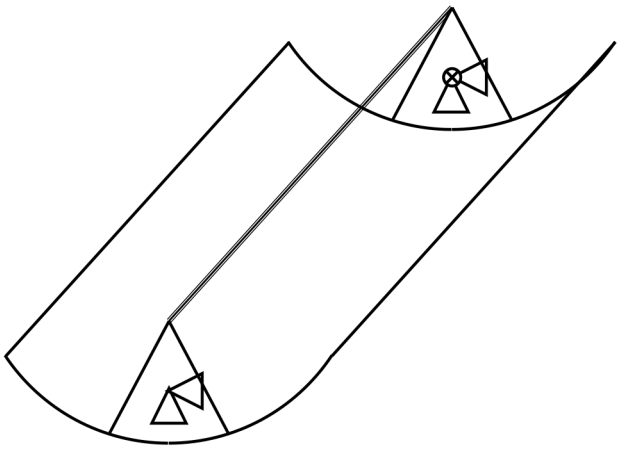

Figure 3 Boundary conditions in operation

The rigid rotation around the axis of the supports has to be prevented as well. In the operating condition, one end is fixed for rotation and the other is free; the blocked end is supposed to be connected to the actuator, if the actuator moves more than one module in the line, the effect of the other modules is simulated applying the calculated torque at the free end.

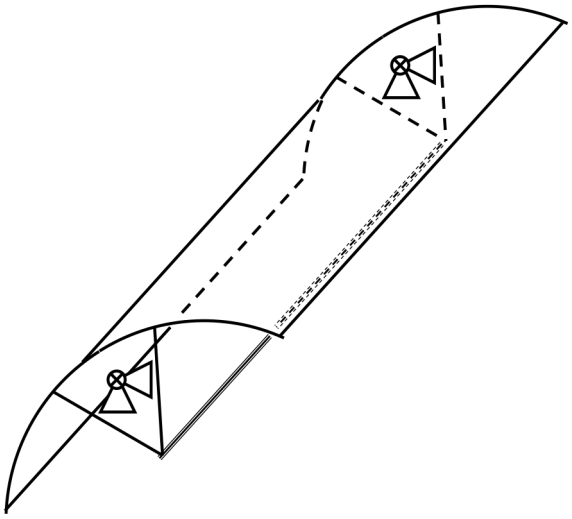

Figure 4 Boundary conditions in protection

When the module is in the protection condition, the rotation is prevented at both ends, in this condition the actuator is not working and the rotation of the trough is avoided by the mechanical blocks on the supports at both ends of the structure.

Results: Gravity load

The structure has been analyzed under the load of its self-weight only, in order to verify the strength and stiffness for two different operative orientations, and in the protection condition.
The structure is simply supported at the two ends, and the rotation around the axis is fixed at one end only.

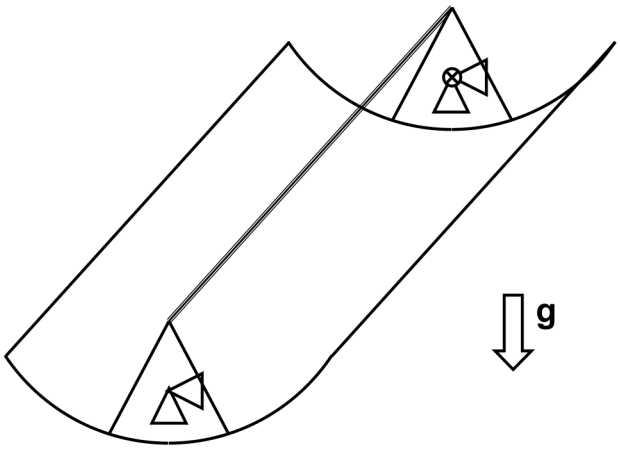

Figure 5 Self-weight load in operating conditions

A single module is analyzed in this step of the analysis, so no additional torque is applied at the trough free end.
All the results will be shown in a reference system fixed to the model, the gravity vector will be rotated and the model is kept in the same position.

Orientation 0°, self weight

Deformation

The deformation of the structure and of the mirrors is shown separately in the following figures. The displacement in the direction of the parabola axis is limited to 22mm (the length of the structure is 12m); this displacement does not affect much the efficiency of the energy concentration, since the absorber tube is linked to the structure.
The most important deformation to be considered is the rotation of the mirror around the axis of the absorber tube; it's value is lower than 2mrad in almost all the mirror surface, except for small areas near the support points, and may be accepted.

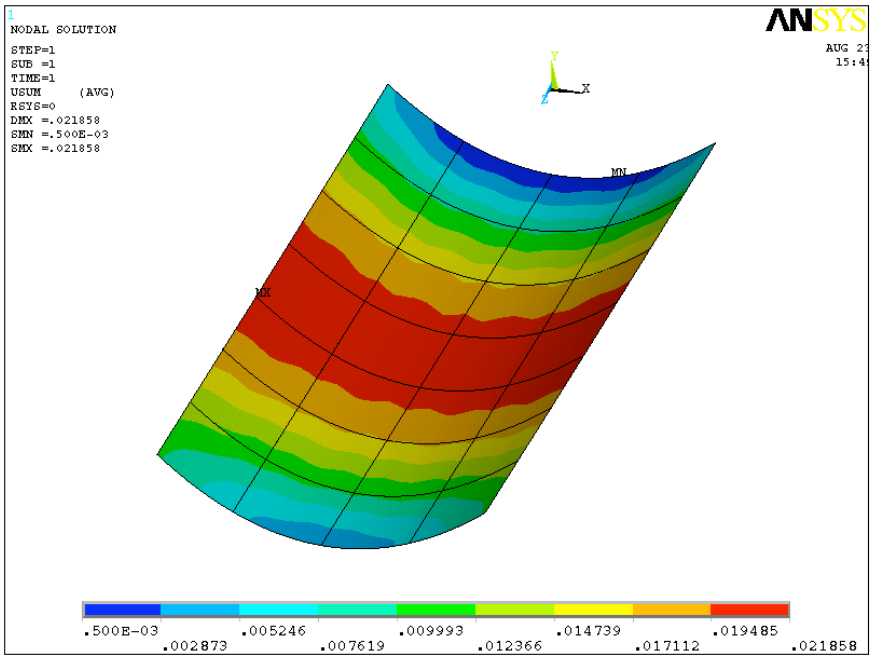

Figure 6 Orientation 0°, self-weight. Displacement magnitude in the mirrors [m]

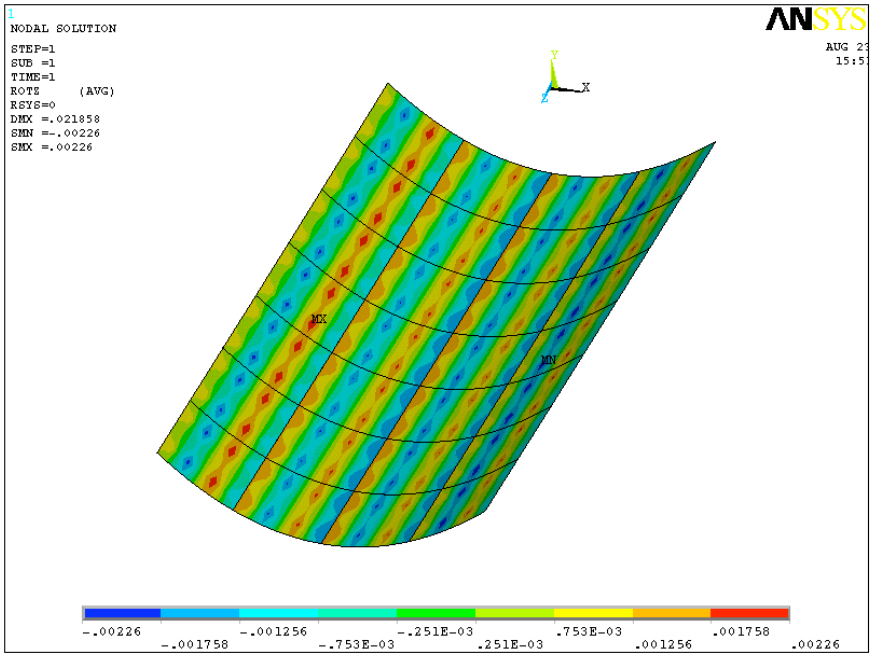

Figure 7 Orientation 0°, self-weight. Rotation around pipe axis (z) in the mirrors [rad]

The displacements in the figure displaying the deformation of the structure has been scaled to better show the structure behavior.

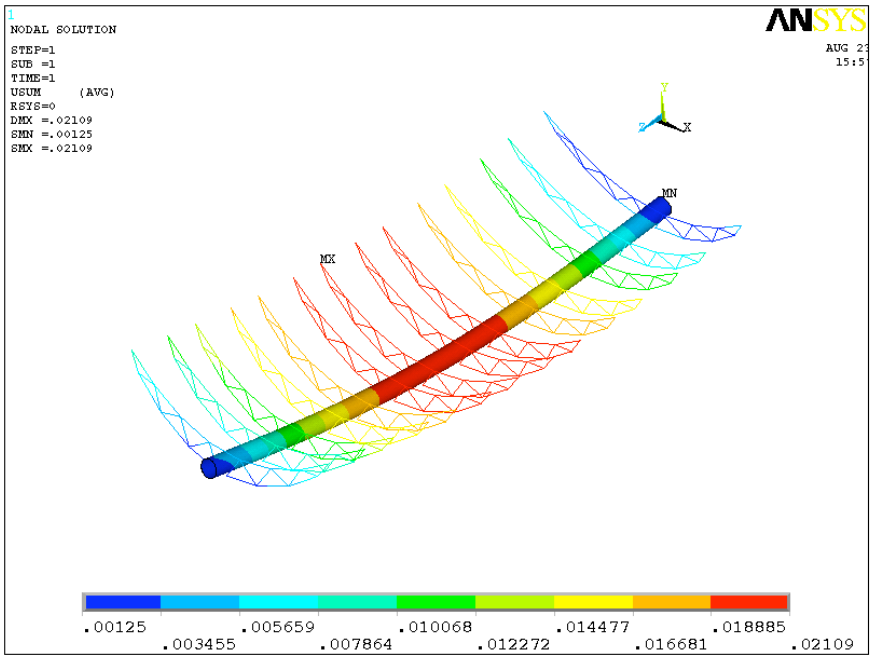

Figure 8 Orientation 0°, self-weight. Displacement magnitude in the steel structure [m] (the displacements are magnified)

Stresses

The figures show separately the Von Mises equivalent stresses in the pipe and the support arms, and the Tresca equivalent stress for the mirrors.
The pipe supports all the load acting on the structure and faces significant stress levels. All the cantilever arms have approximately the same loads acting and face the same stress levels. The stresses in the mirrors are not low when compared to the mirror strength and are

concentrated in the support points, the stress results for the mirrors have to be considered has a rough approximation since a more detailed model have to be adopted for the mirror analysis.

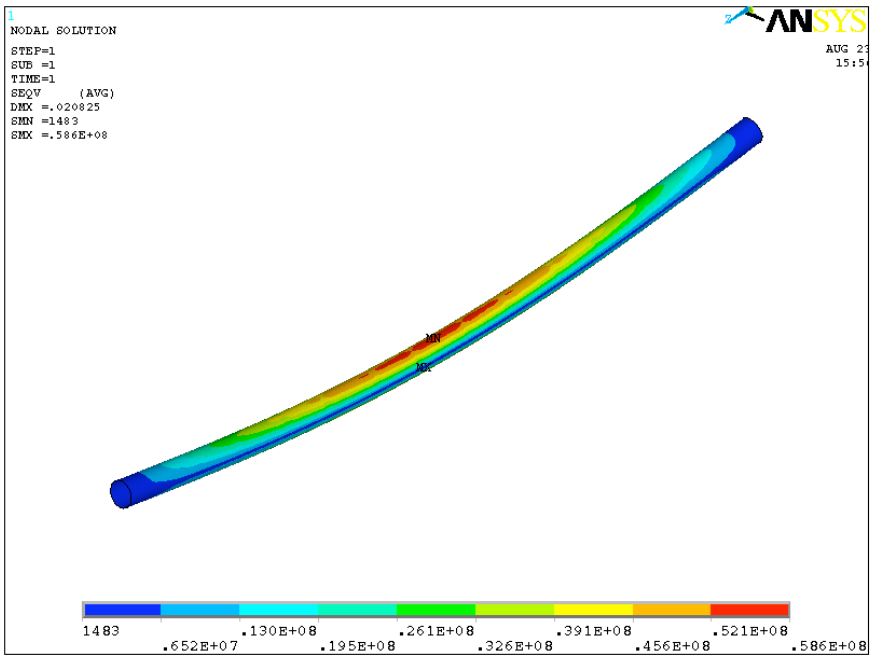

Figure 9 Orientation 0°, self-weight. Equivalent stress intensity in the pipe [Pa] (the displacements are magnified)

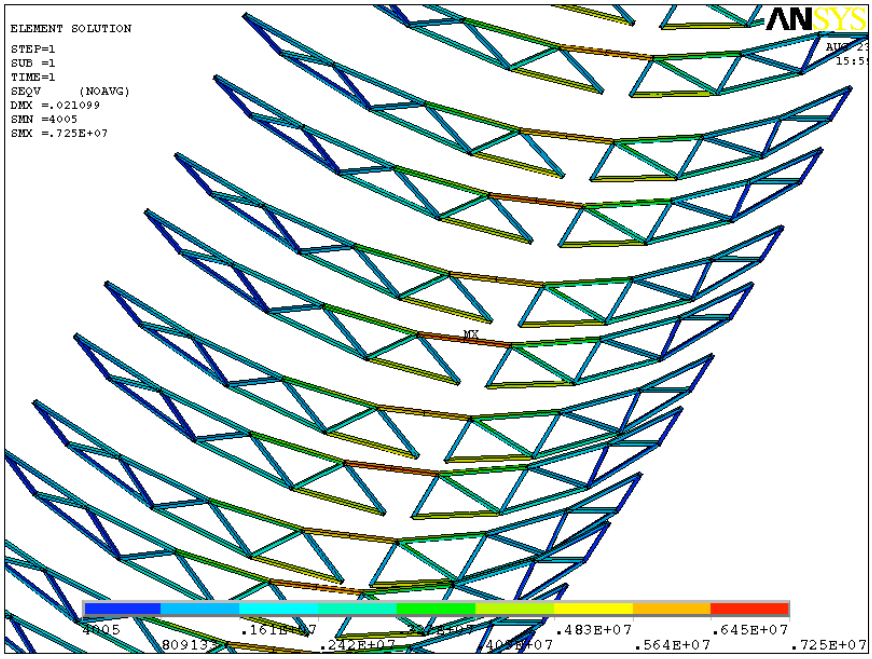

Figure 10 Orientation 0°, self-weight. Equivalent stress intensity in the arms [Pa] (the displacements are magnified)

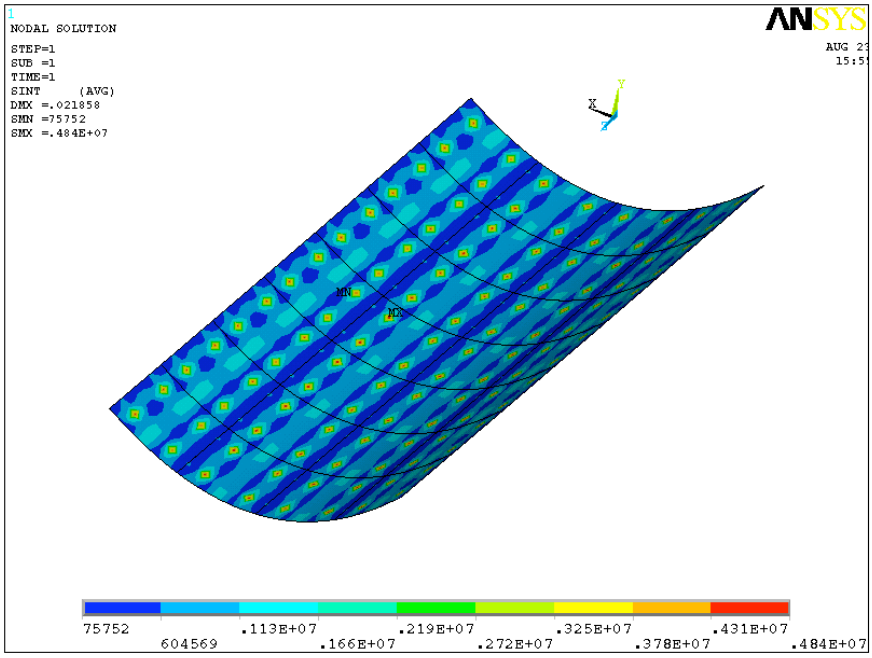

Figure 11 Orientation 0°, self-weight. Equivalent stress intensity in the mirrors [Pa]

Reaction forces

The structure is simply supported; only a vertical force of 8910N is applied to each support.

Orientation 30°, self weight

Deformation

The following figures show the deformation and rotation around the z axis of the mirrors, and the deformation of the steel structure.
The maximum displacement value is approximately 23mm in this orientation too, as expected, and this does not affect the concentration efficiency.
The rotation of the mirror surface around the absorber tube axis reaches a maximum value of 3mrad. This peak is anyway limited to a small portion of the overall surface whereas the rest of the reflective surface is well below the 2mrad reference.

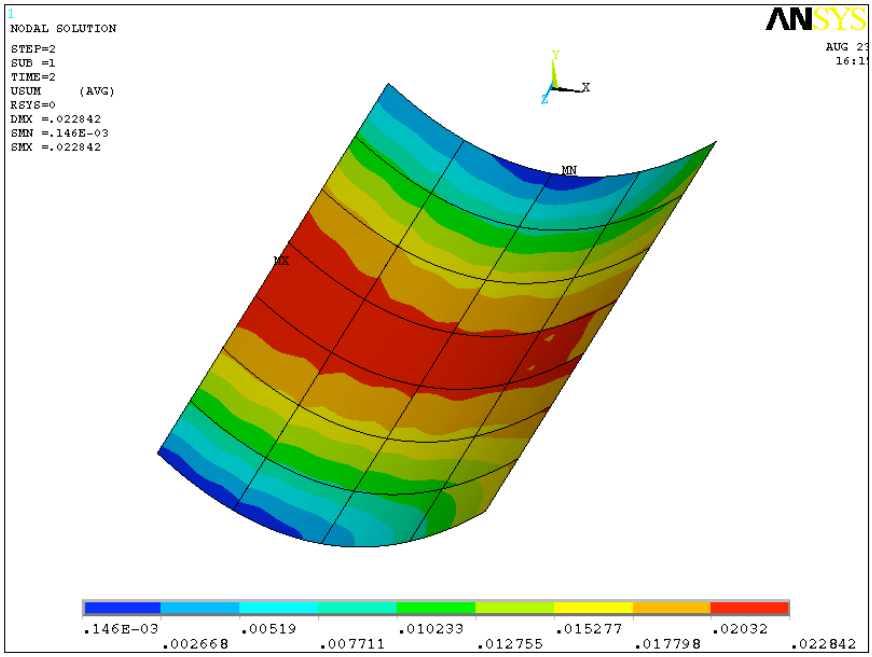

Figure 12 Orientation 30°, self-weight. Displacement magnitude in the mirrors [m]

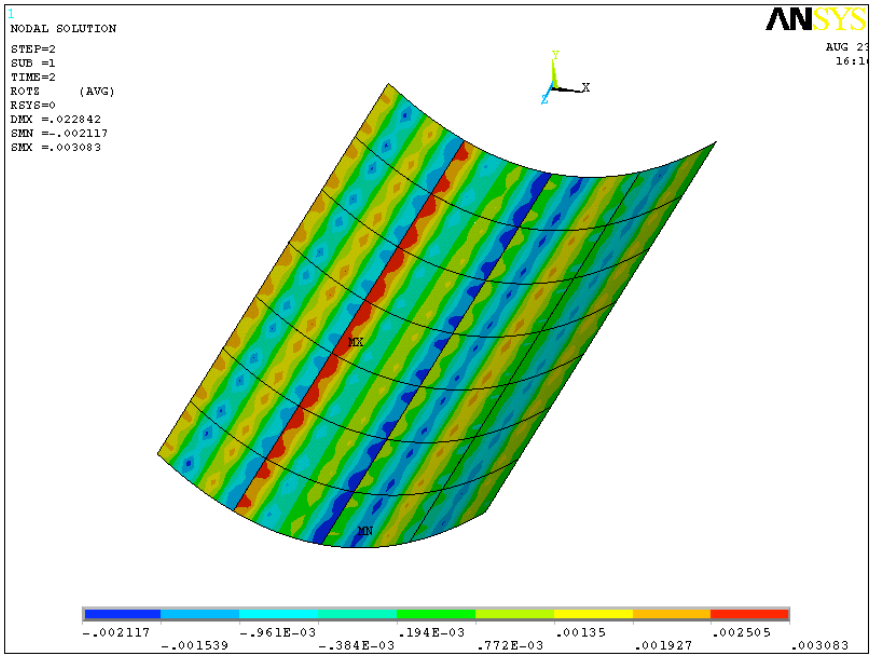

Figure 13 Orientation 30°, self-weight. Rotation around pipe axis (z) in the mirrors [rad]

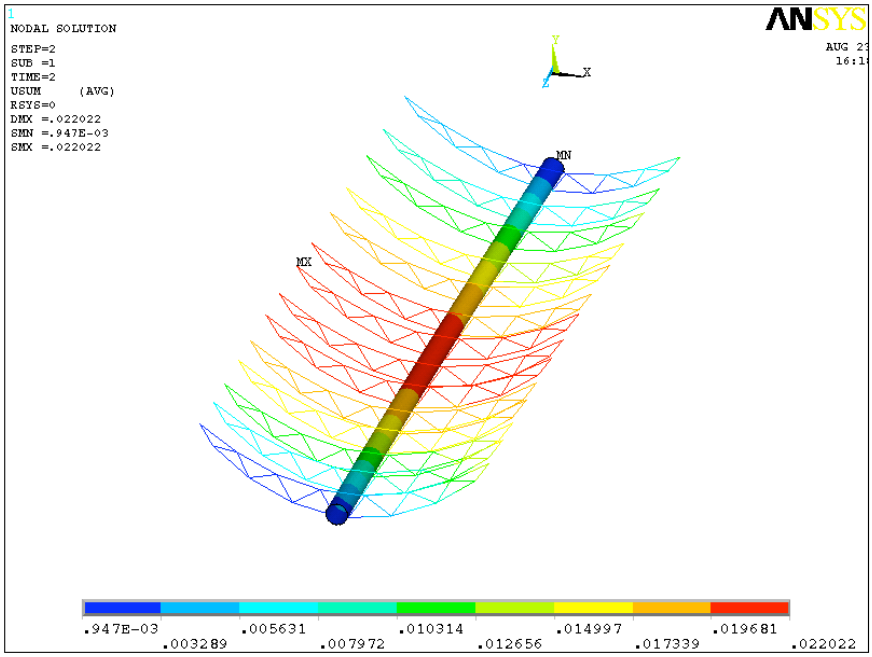

Figure 14 Orientation 30°, self-weight. Displacement magnitude in the steel structure [m]

Stresses

The Von Mises equivalent stresses in the steel structure and the Tresca equivalent stresses for the mirrors are shown in the following figures.
The stress intensity is similar to that found in the 0° orientation of the trough.
The stresses on the cantilever arms and on the mirrors are relatively more intense, but not significantly.

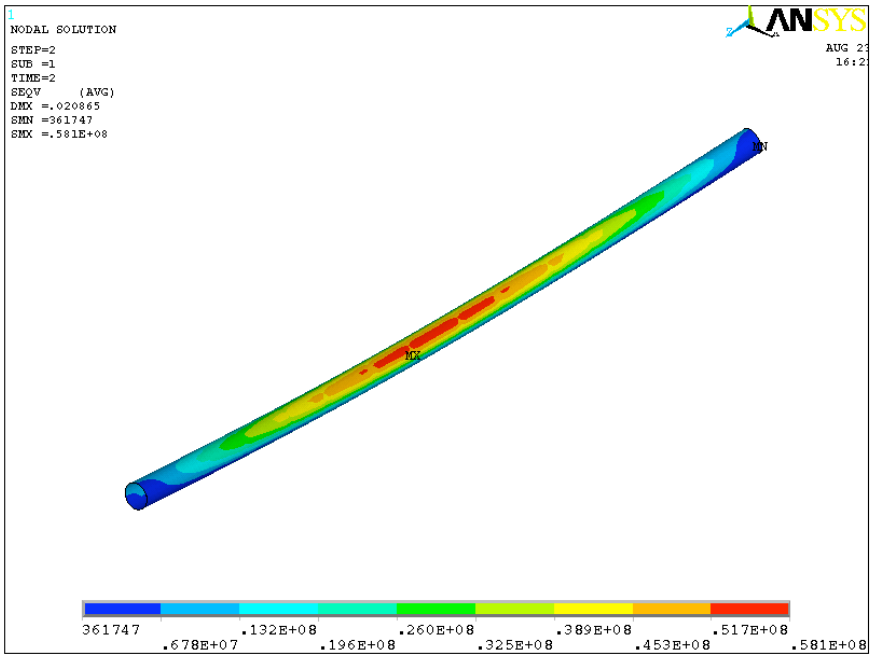

Figure 15 Orientation 30°, self-weight. Equivalent stress intensity in the pipe [Pa] (the displacements are magnified)

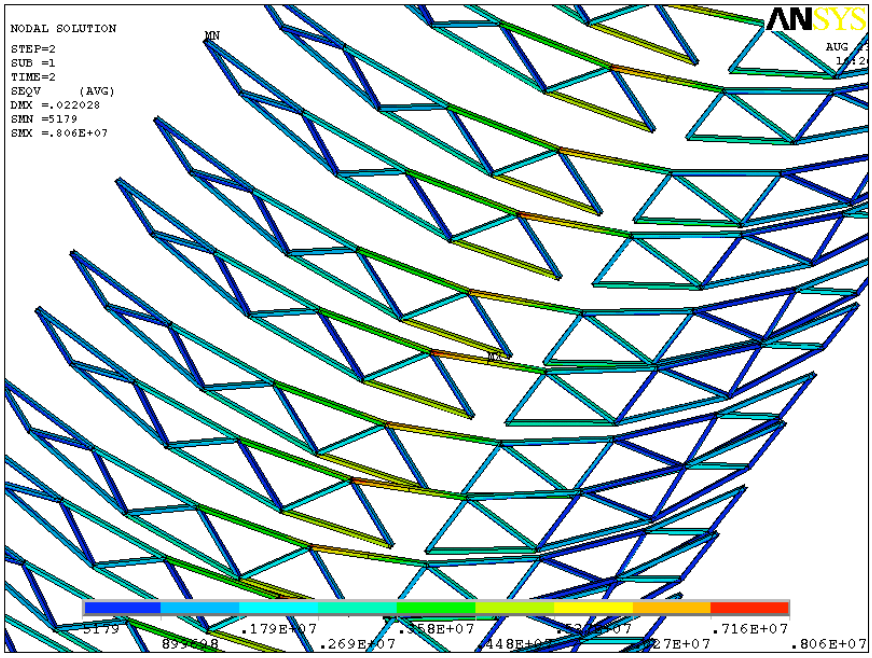

Figure 16 Orientation 30°, self-weight. Equivalent stress intensity in the arms [Pa] (the displacements are magnified)

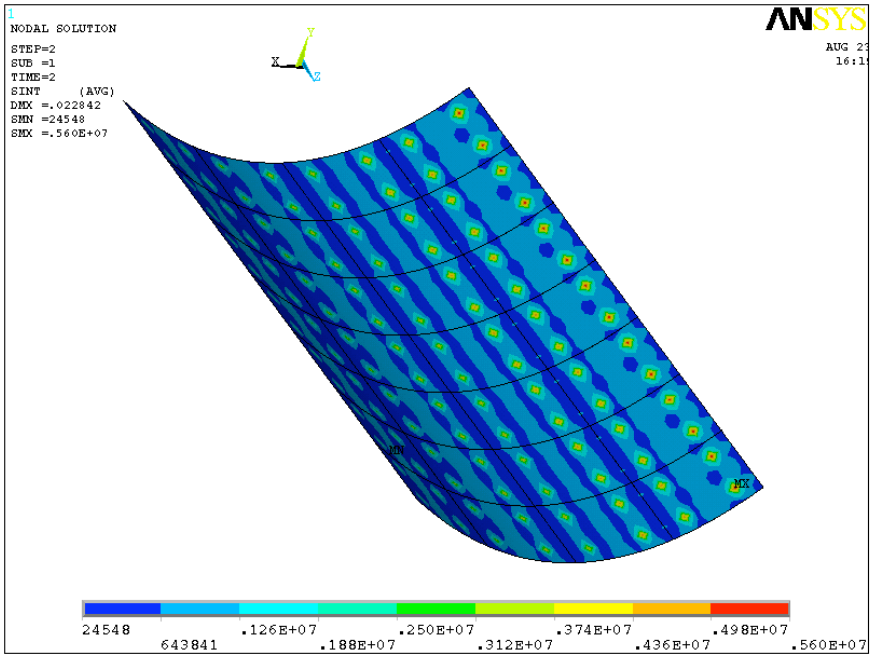

Figure 17 Orientation 30°, self-weight. Equivalent stress intensity in the mirrors on the back surface [Pa]

Reaction forces

The structure is simply supported, the vertical force on each support is 8910N and since the axis of rotation is not coincident with the centre of gravity a torque of 153Nm is applied at one end.

Orientation 210°, gravity load

Deformation

The deformation is not of interest since the trough is not working.

Stresses

The resulting stresses in this orientation are identical to those found for the 30° position.

Reaction forces

The structure is simply supported, the vertical force on each support is 8910N and since the axis of rotation is not coincident with the centre of gravity a torque of 152.83Nm is applied at one end.

Results: Wind loads

The main load on the structure is due to the action of the wind. As mentioned the trough line may be seen as a wing attached to the ground, it will be subject to high loads in both operating and emergency conditions.
When the line is working the wind will affect the stress level of the structure and will also cause a deformation of the reflective surface that may influence the efficiency of the system.
When very high winds are acting the structure is rotated in an emergency position that protects the absorber tube. The structure should be strong enough to withstand these loads without damage.

Orientation 210°, gravity load and wind 30m/s

When weather conditions do not allow power production, the trough is rotated in the protection position, at an angle of 210° and facing the wind with the back side of the mirrors.
The structure will be subject to the highest load in this position. The model is verified under the action of the gravity load and of a wind of 30m/s acting on the surface.
The structure is simply supported at the two ends, and the rotation around the axis is fixed at both ends.

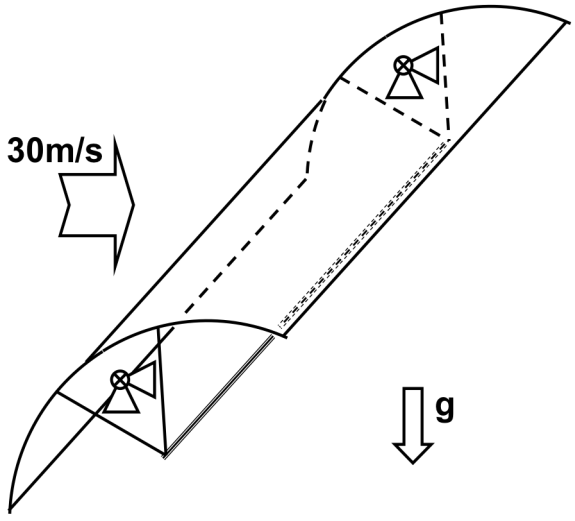

Figure 18 Self-weight load and high wind in protection condition.

A CFD numerical simulation has calculated the fluid dynamics of the wind around the parabola, and the pressure acting on the back mirror surface is shown in the following figure.

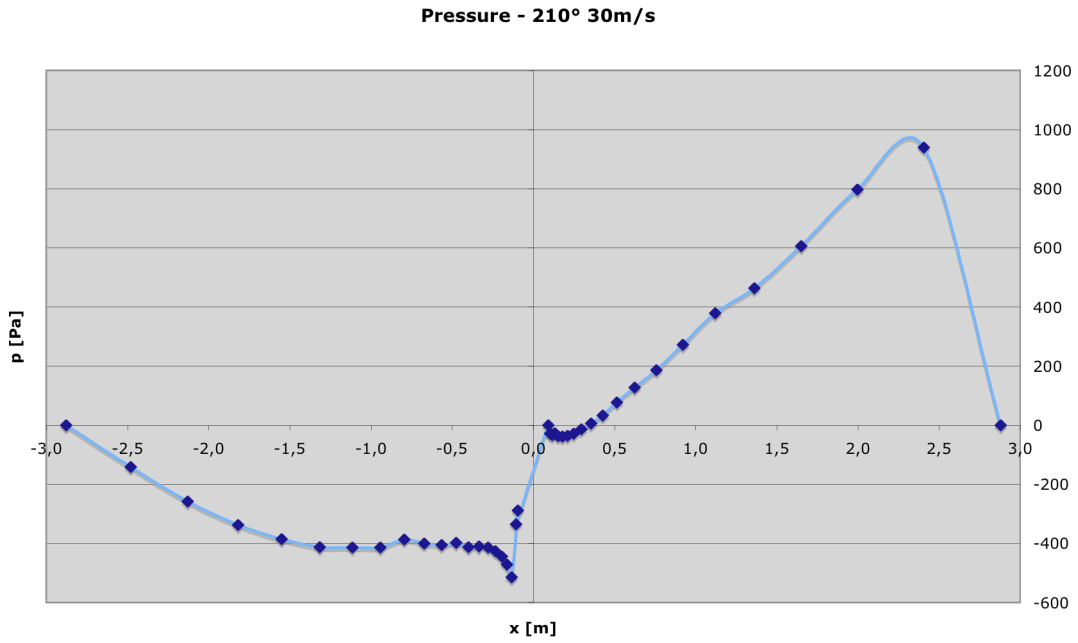

Figure 19 Pressure on the mirror external surface due to a 30m/s wind as results from CFD simulation for a 210° orientation

Deformations

The structure bends as an effect of the self-weight and of the wind; the displacement magnitude and the rotation around the z axis of the structure are shown in the following figures. No deformation limit is required in this condition and the results are shown only for the sake of completeness.

The maximum displacement of 56mm is found on the mirrors facing the wind, where the maximum pressure is acting.

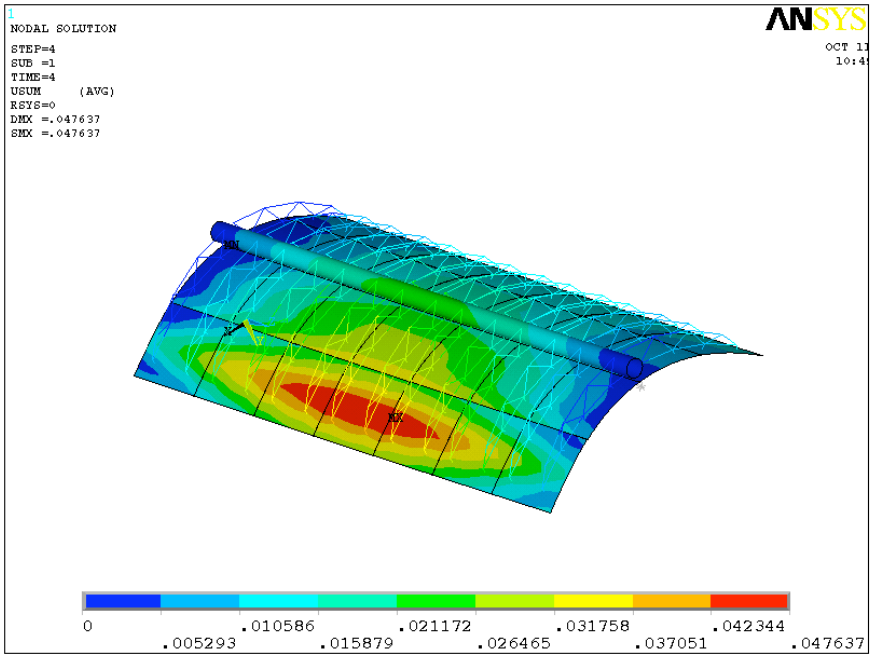

Figure 20 Orientation 210°, self-weight and wind 30m/s. Displacement magnitude in the model [m]

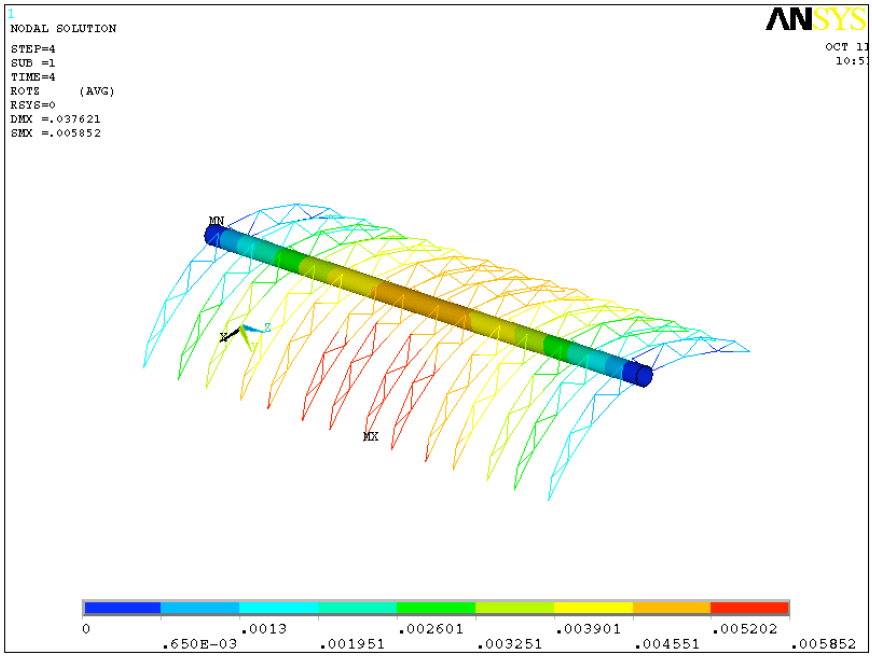

Figure 21 Orientation 210°, self-weight and wind 30 m/s. Rotation around pipe axis (z) in the steel stucture [rad]

Stresses

The figures show separately the Von Mises equivalent stresses in the pipe and the support arms, and the Tresca equivalent stress for the mirrors.
The pipe is here subject to a bending and twisting loading condition. The maximum bending moments are located at the center of the beam whereas the maximum twisting moments are at the ends; the distribution of the equivalent stress intensity is rather uniform, with a maximum value of 68MPa at the central section.
All the cantilever arms have approximately the same stress distribution and intensity. The maximum value resulting is 37MPa.
High stresses are found on the mirrors, in particular on the support points of the first row. The stress result is not accurate enough since a more detailed model would be required to solve the stress concentration in the supports with accuracy. A detailed model of the mirror will be analyzed.

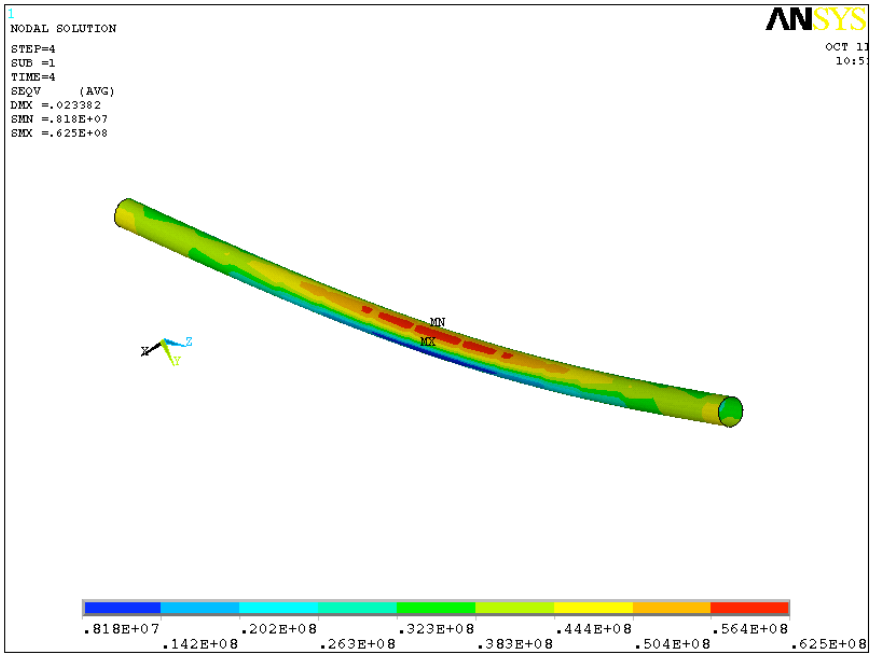

Figure 22 Orientation 210°, self-weight and wind 30m/s. Equivalent stress intensity in the pipe [Pa] (the displacements are magnified)

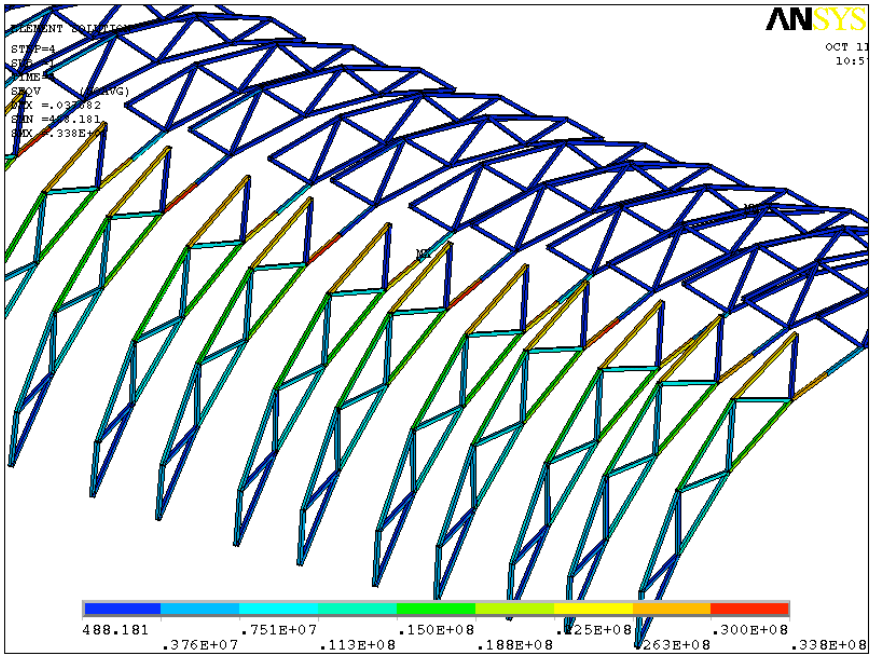

Figure 23 Orientation 210°, self-weight and wind 30m/s. Equivalent stress intensity in the arms [Pa] (the displacements are magnified)

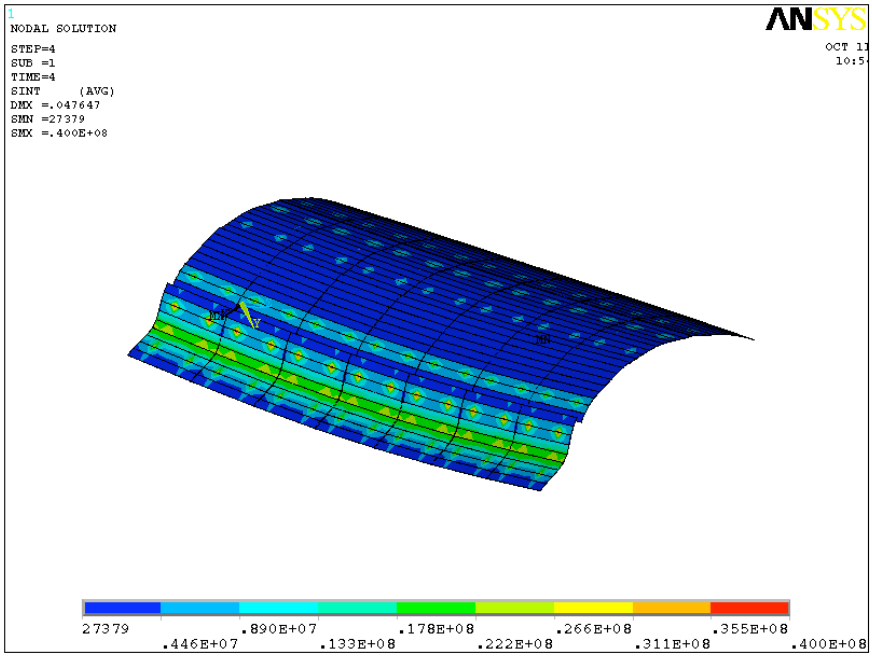

Figure 24 Orientation 210°, self-weight and wind 30m/s. Equivalent stress intensity in the mirrors [Pa] (the displacements are magnified)

Reaction forces

The structure is simply supported; the loading on each support is the same and is composed by a vertical force of 7108N, a lateral (drag force) of 7508N and a torque of 28833Nm. The vertical force is lower than that due to the self-weight only: the wind has a lifting effect on the structure.

Orientation 0°, self weight and transverse wind at 15m/s for a single module

In operating conditions the reflective surface should concentrate the solar energy on the absorber tube, in any angle between -60° and +60° with respect to the vertical direction. The efficiency of the concentrator is affected by the deformation of the reflective surface; it is therefore necessary to verify the stiffness of the structure and its strength for different orientations and under the action of the wind. The wind intensity of 15m/s is very high; the trough could hardly be operating in these conditions. Anyway the structure should still be strong enough to rotate to the protection position and the actuator should give enough torque to rotate the structure.
The deformations and stresses are proportional to the square of the wind velocity, therefore the deformations at 7m/s could be easily estimated dividing by a factor of 4 the results obtained.
The structure is simply supported at the two ends, and the rotation around the axis is fixed at one end.

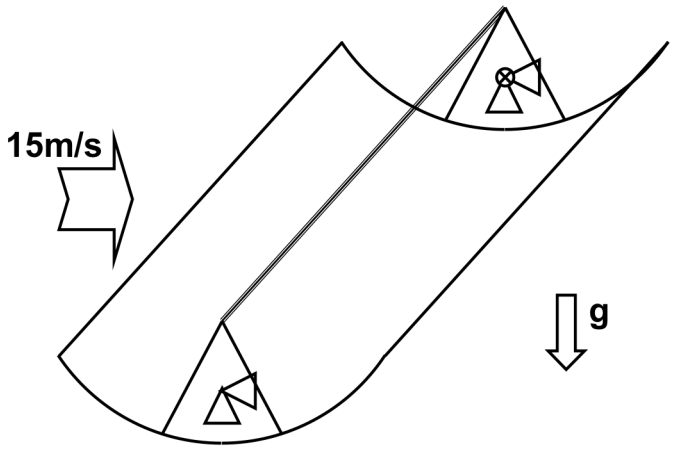

Figure 25 Self-weight load and 15m/s wind in operating condition.

A CFD numerical simulation has calculated the fluid dynamics of the wind around the parabola, and the pressure acting on the mirror surface is shown in the following figure.

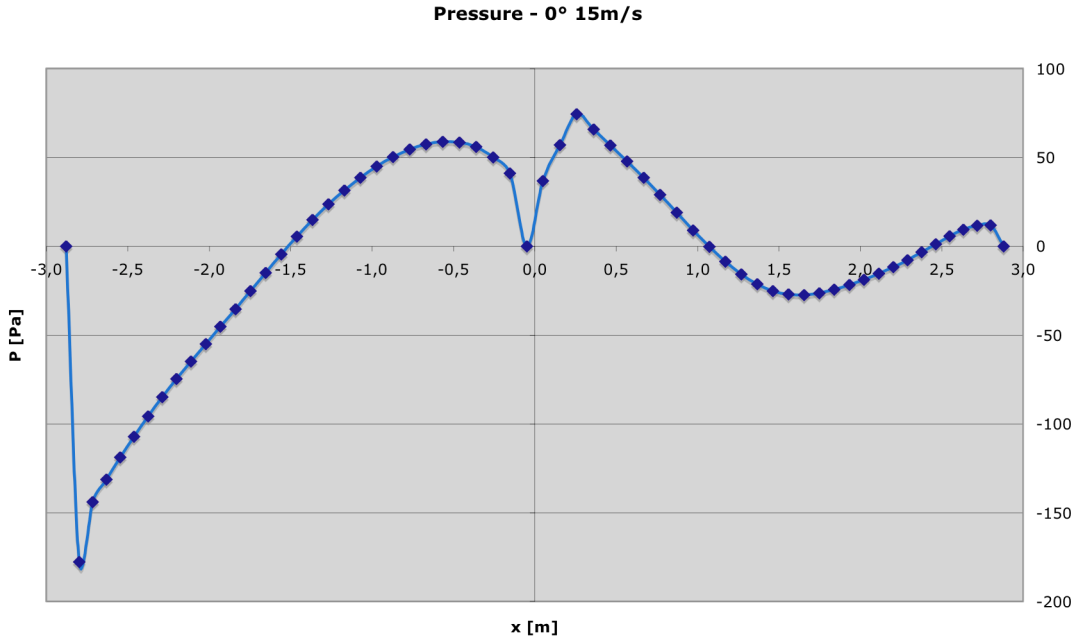

Figure 26 Pressure on the mirror internal surface due to a 15m/s wind as results from CFD simulation for a 0° orientation

Deformation

The following figures show the deformations of the mirrors and the steel structure. The maximum displacement is approximately 24mm on the mirror surface and 3 mm on the structure. The results are similar to those found when the self-weight only was applied. The deformation is not along the parabola axis but has a component in the transverse direction due to the wind effect, this effect does not influence the solar collector efficiency since the absorber tube is linked to the structure and has the same displacements.

The wind effect is evident on the mirror surface rotations around the absorber tube axis, which are much higher then those found for the self-weight load only. There is a (limited) portion of the reflecting surface where the rotation reaches 5mrad. It is interesting to notice that the rotations in the structure is limited, the structure appears to be stiff, and the rotation is mainly

due to the deformation of the mirror, at least in this load case when a single module per side of the actuator is considered.

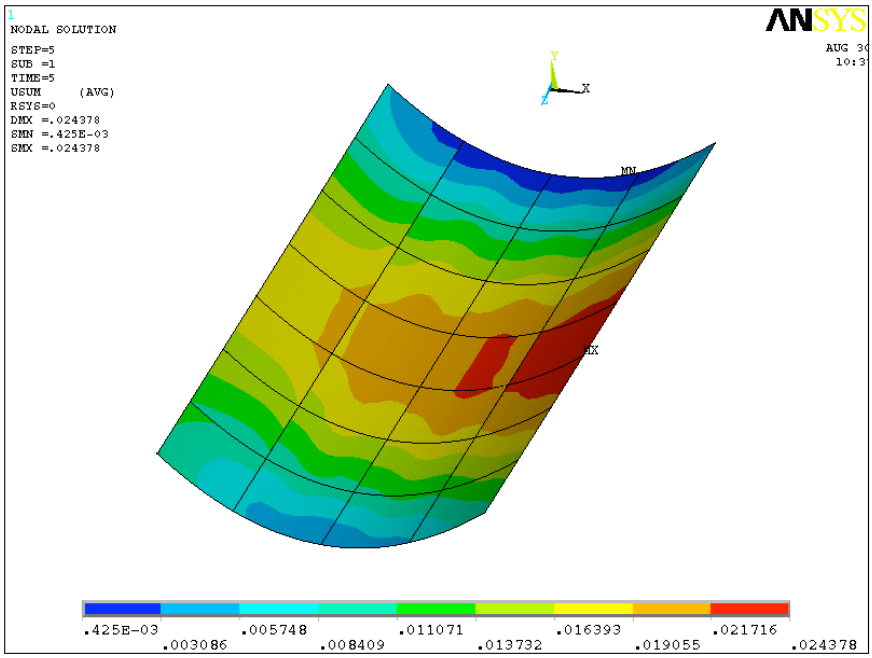

Figure 27 Orientation 0°, self-weight and wind 15m/s, single module. Displacement magnitude in the mirrors [m]

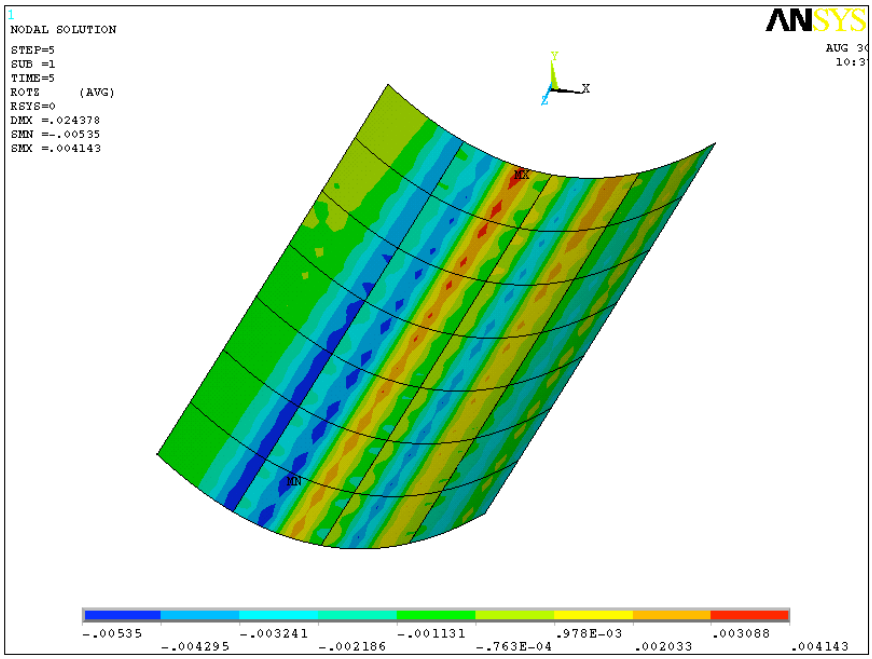

Figure 28 Orientation 0°, self-weight and wind 15m/s, single module. Rotation around pipe axis (z) in the mirrors [rad]

The displacements in the figure displaying the deformation of the structure has been scaled to better show the structure behavior.

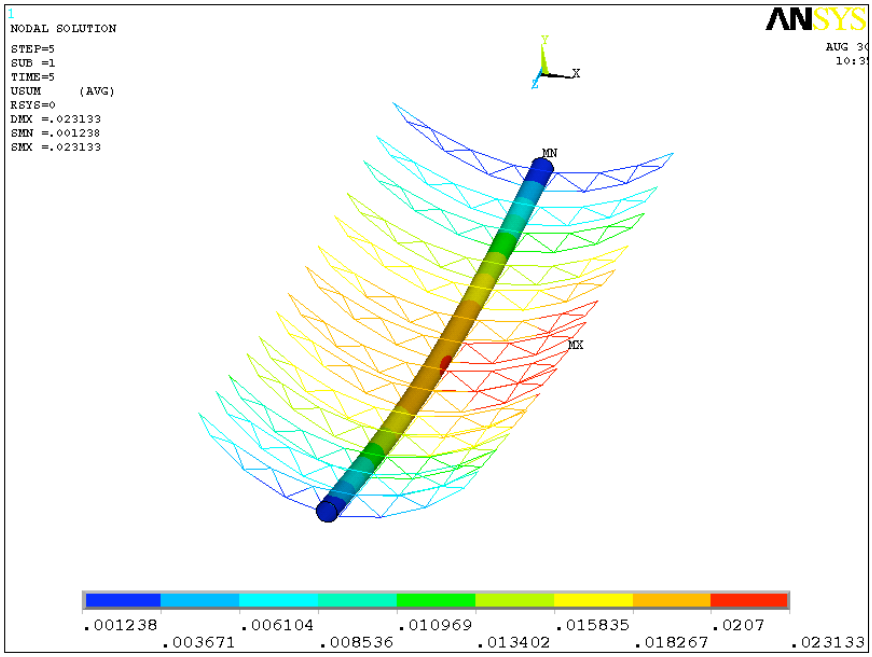

Figure 29 Orientation 0°, self-weight and wind 15m/s, single module. Displacement magnitude in the steel structure [m] (the displacements are magnified)

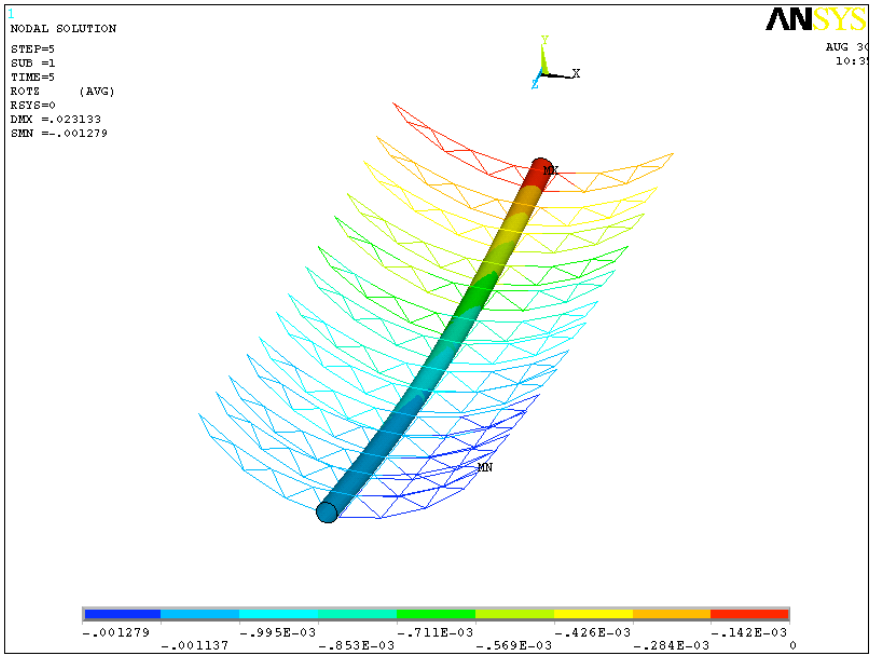

Figure 30 Orientation 0°, self-weight and wind 15m/s, single module. Rotation around pipe axis (z) in the steel structure [rad] (the displacements are magnified)

Stresses

The figures show separately the Von Mises equivalent stresses in the pipe and the support arms, and the Tresca equivalent stress for the mirrors.
The stress intensity in the structure is similar to that found in the previous load cases: pipe bending is the predominant effect, the torsion appears not very high in this case, and the stresses are mainly directed along the pipe axis. The stresses in the cantilever arms are again limited with a distribution similar to that described for the self-weight only load case.

The stresses in the mirrors are not low when compared to the mirror strength and are concentrated in the support points, the stress results for the mirrors have to be considered has a rough approximation since a more detailed model have to be adopted for the mirror analysis.

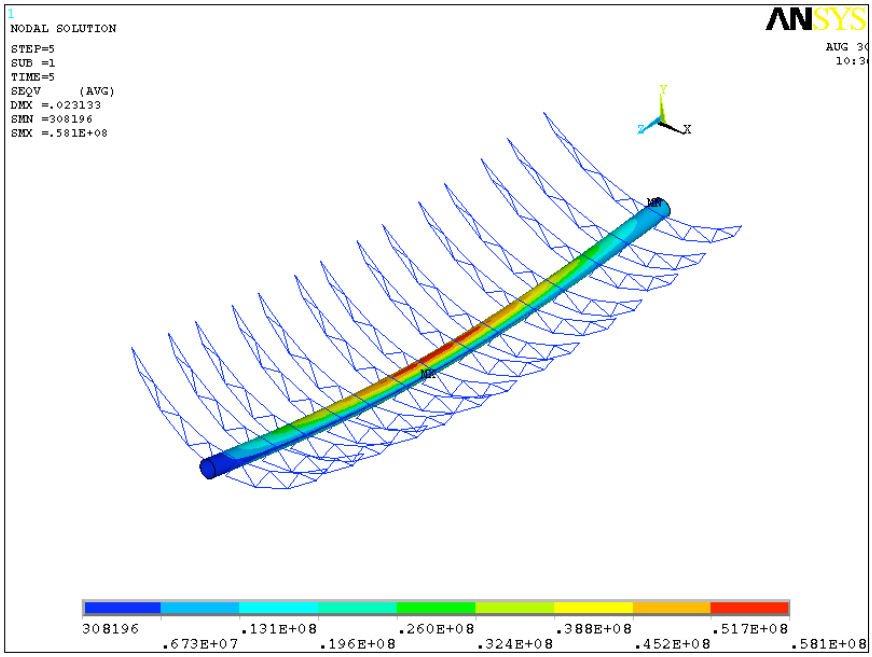

Figure 31 Orientation 0°, self-weight and wind 15m/s, single module. Equivalent stress intensity in the pipe [Pa] (the displacements are magnified)

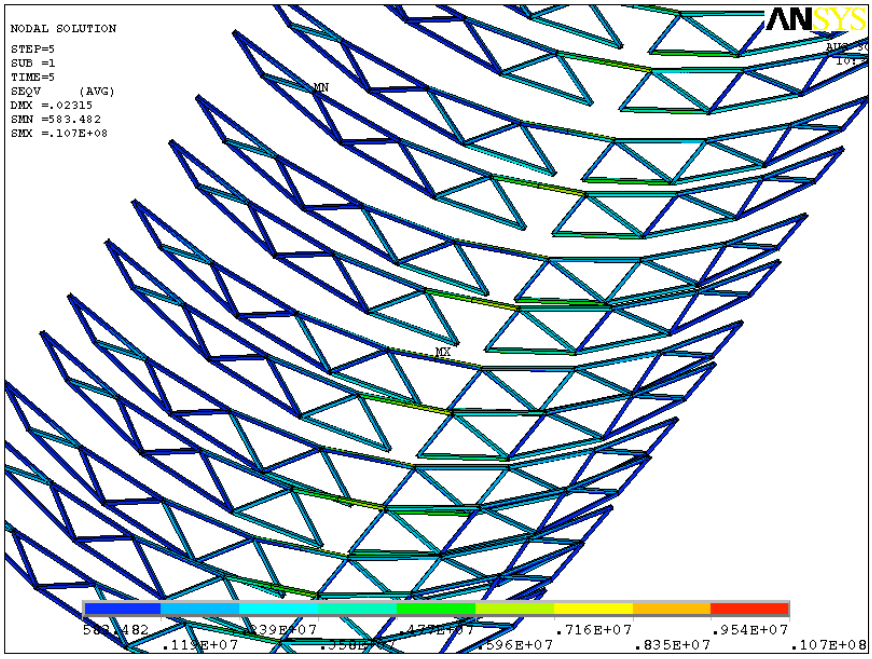

Figure 32 Orientation 0°, self-weight and wind 15m/s, single module. Equivalent stress intensity in the cantilever arms [Pa] (the displacements are magnified)

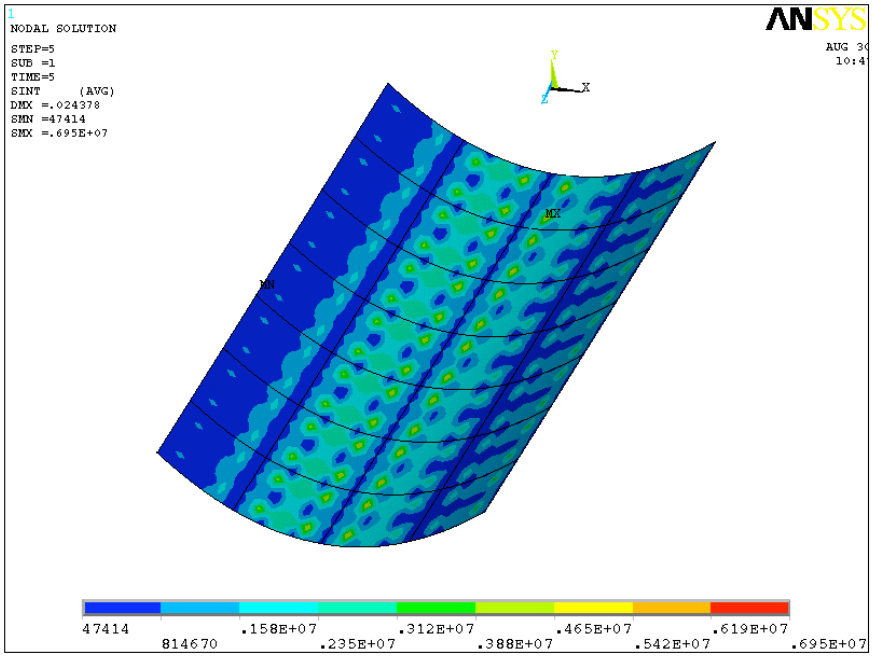

Figure 33 Orientation 0°, self-weight and wind 15m/s, single module. Equivalent stress intensity in the mirrors [Pa]

Reaction forces

The structure is simply supported; the same reaction forces are acting on the supports: the vertical force is 8824N and the transverse force is 312N. The torque required to the actuator is 2742Nm. The rotation at the end of the structure is 1.1mrad.

Orientation 0°, self weight and transverse wind at 15m/s, for a two modules per side configuration

In this configuration two modules are attached at each side of the actuator, the total length of the line is therefore approximately 48m.
Two separate analyses were run for each module of the side, with different boundary conditions. The first module is linked to the actuator, at one end the rotation is fixed and at the other end the torque due to the second module is applied. The second module has one end free to rotate, the rotation of the other end is fixed to the value of the “free” end of the first module.
The structures are simply supported with respect to bending, and are subject to the action of gravity and wind. The wind pressure results from the CFD simulation already mentioned.

Deformation

The following figures show the deformations of the mirrors and the steel structure in the configuration of two modules per side connected (four module for each actuator).
The distribution and amplitude of the displacements of the mirror surface is mainly influenced by the bending of the structure; the results are therefore similar to those found in he single module case. The torsion of the structure has an influence as well, and the displacements of the reflecting surface are higher for the module not directly connected to the actuator.

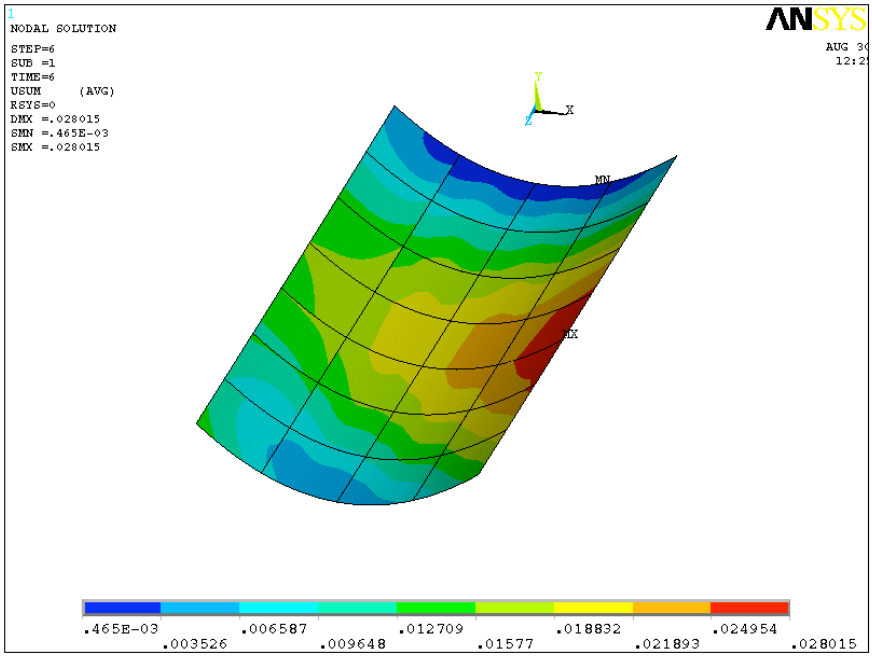

Figure 34 Orientation 0°, self-weight and wind 15m/s, two modules per side. Displacement magnitude in the mirrors of the first module [m]

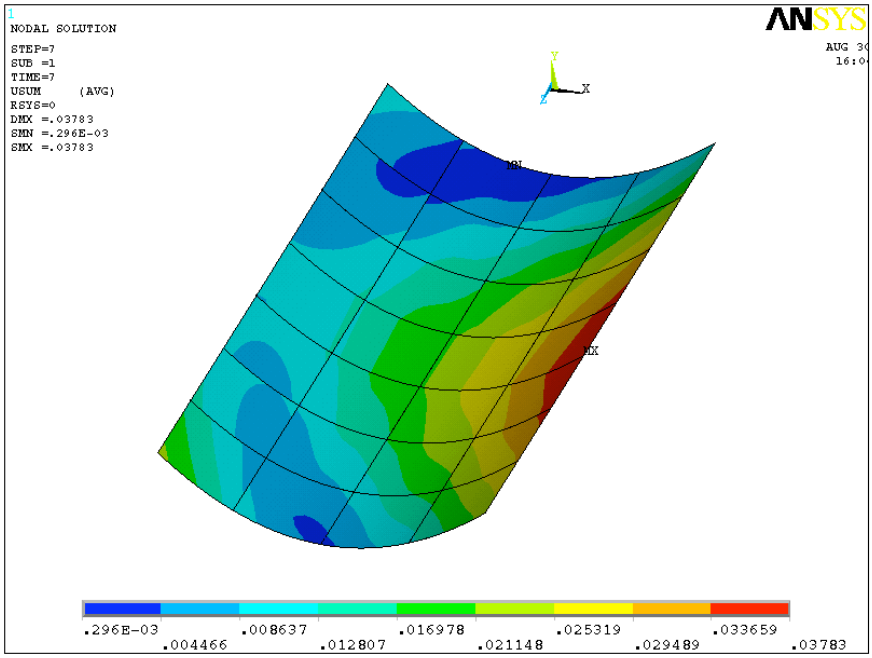

Figure 35 Orientation 0°, self-weight and wind 15m/s, two modules per side. Displacement magnitude in the mirrors of the second module [m]

The connection of the two modules has an important effect on the rotations of the reflective surface around the absorber tube axis. The values of the rotations are much higher with respect to the values found in the single module case.

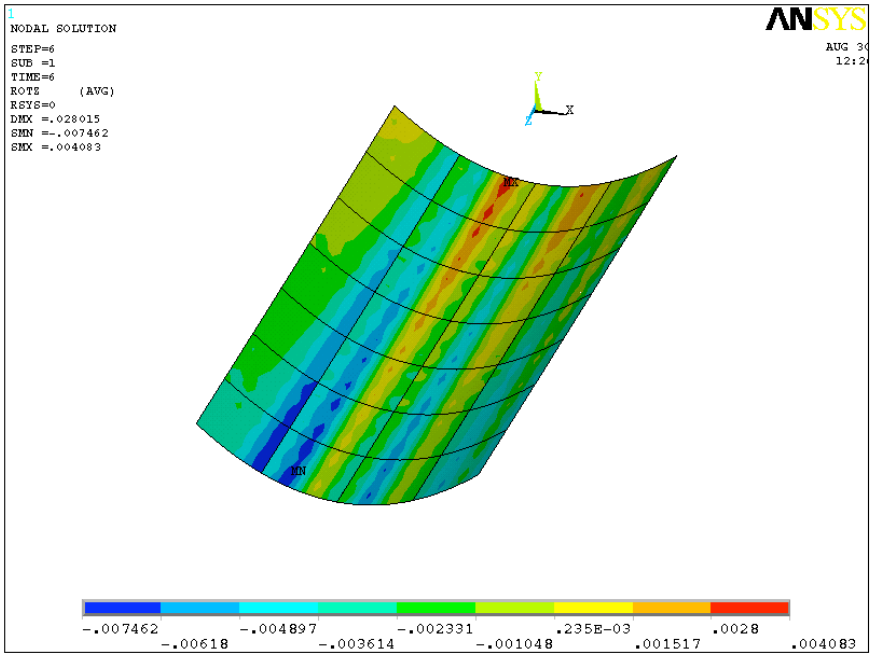

Figure 36 Orientation 0°, self-weight and wind 15m/s, two modules per side. Rotation around pipe axis (z) in the mirrors of the first module [rad]

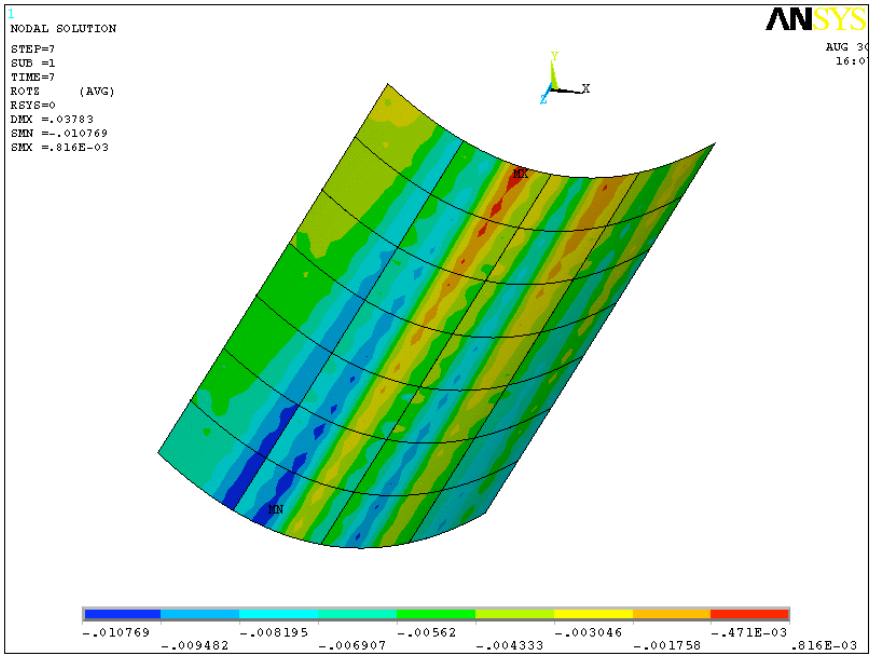

Figure 37 Orientation 0°, self-weight and wind 15m/s, two modules per side. Rotation around pipe axis (z) in the mirrors of the second module [rad]

The distribution of the rotation on the surface is similar, but on the second module, far from the actuator, there is the effect of the rotation of the structure. The maximum resulting rotations are remarkable, almost reaching 11mrad in some portions of the second module reflective surface. The following figures show the rotations of the steel structure of the two modules, the displacements are magnified.

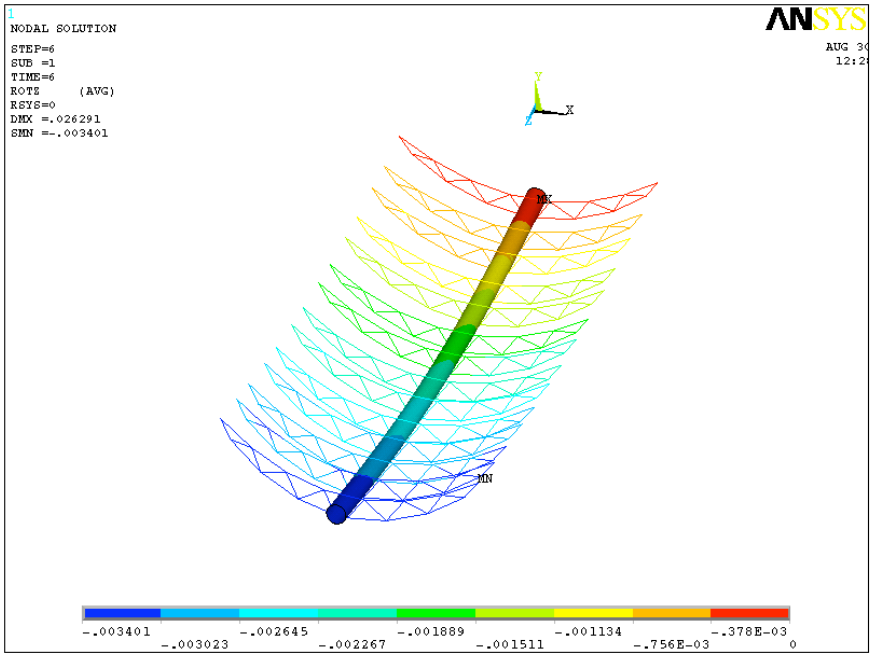

Figure 38 Orientation 0°, self-weight and wind 15m/s, two modules per side. Rotation around pipe axis (z) of the structure of the first module [rad] (the displacements are magnified)

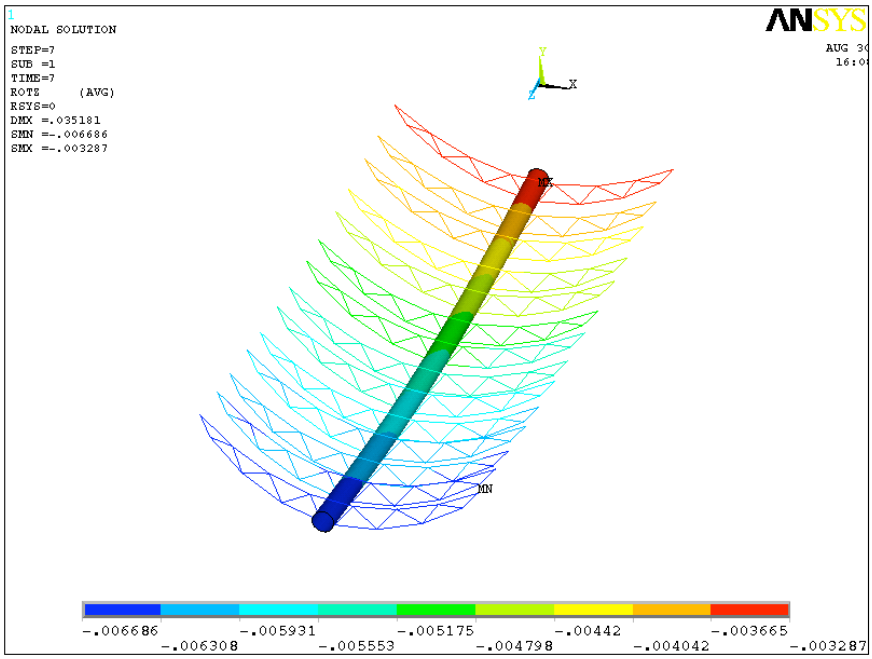

Figure 39 Orientation 0°, self-weight and wind 15m/s, two modules per side. Rotation around pipe axis (z) of the structure of the second module [rad] (the displacements are magnified)

The efficiency of the collector in these conditions is greatly reduced, it may be enhanced adopting a stiffer absorbing tube, and stiffer mirrors as well.

Stresses

The loads acting on the second module of the row, the one far from the actuator are the same acting on the single module; as a consequence the stresses will be equal as well. The loads acting on the first module also include the torque due to the second module of the row. The

stresses on the structure could therefore be higher with respect to the single module case and are shown in the following figure.

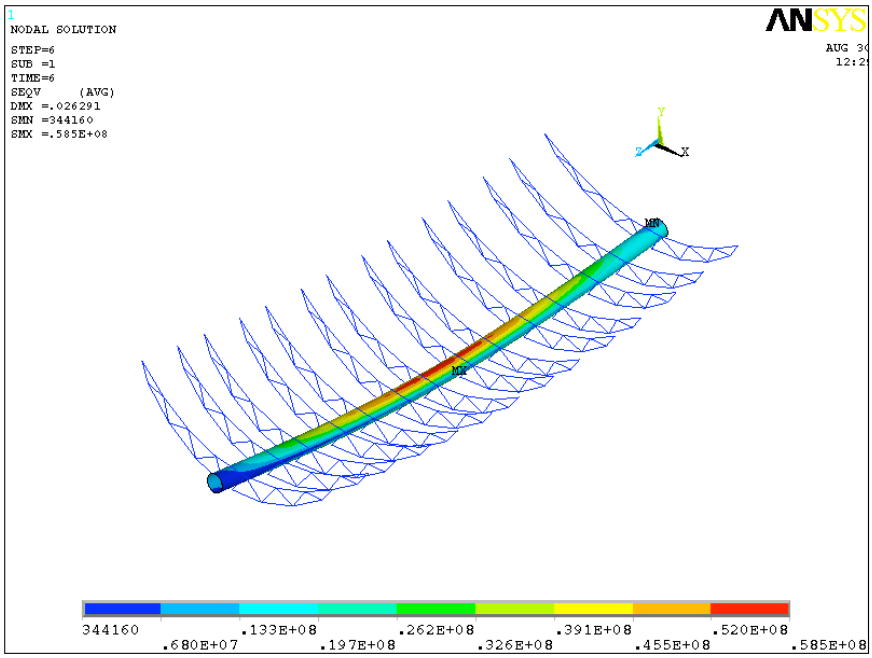

Figure 40 Orientation 0°, self-weight and wind 15m/s, two modules per side. Equivalent stress intensity in the pipe for the first module [Pa] (the displacements are magnified)

The bending load is still the more important when compared to the torque, and the stress on the pipe are clearly due to the bending moments. The maximum equivalent stress is still 59MPa as found for the single module example.

Reaction forces

The structures are simply supported; the reaction forces are the same for each module: the vertical force is 8824N and the transverse force is 312N; the shared support will be subject to the reactions of both module and the force intensity will be doubled. The torque required to the actuator is 5478Nm per side, and almost 11kNm for the 48m long trough line. The rotation at the end of the first module is 3.278mrad and 6.572mrad at the end of the second module.

Buckling analysis

Reference model

Some parts of the structure of the module are subject to high compressive loads that may cause the buckling of the structure.
A buckling analysis of the whole module has shown that local structural instabilities may appear on the structural tube. These local instabilities cannot be judged properly since they are strongly dependent by the connections between the different portions of the model, and cannot be considered as affordable.
A detailed model of the support truss has therefore been prepared and analyzed with respect to its buckling behavior.
The following figure shows the first buckling mode of this model when the 30m/s wind is applied and the orientation of the trough is 210°.

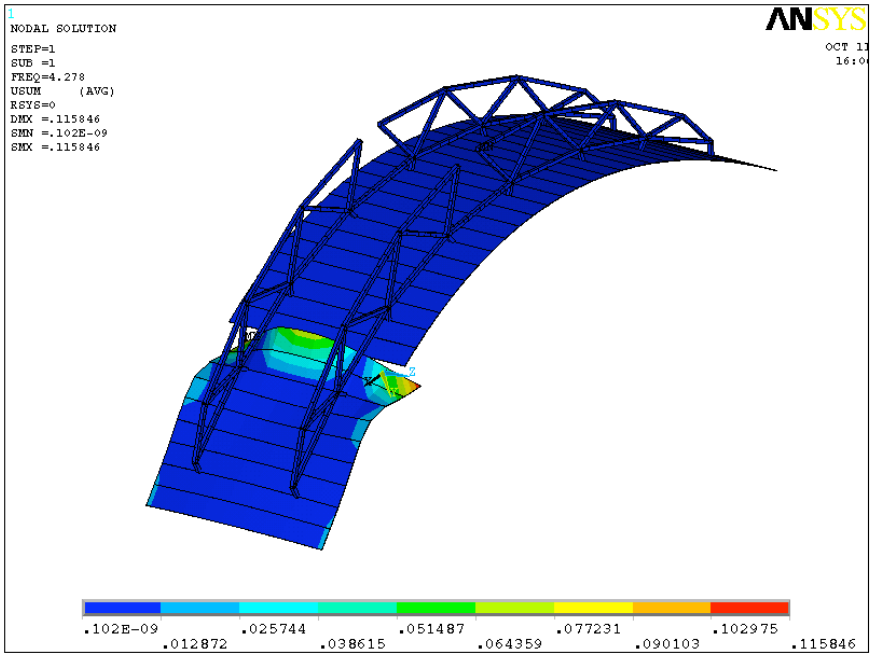

Figure 41 Orientation 210°, self-weight and wind 30m/s. First buckling mode, multiplying factor 4.3

The first buckling mode results to be confined to the mirror surface, it results anyway that it should be necessary a load 4.3 times higher than the one applied to cause this instability.
The first interesting mode in the trough protection position is shown in the following figure.

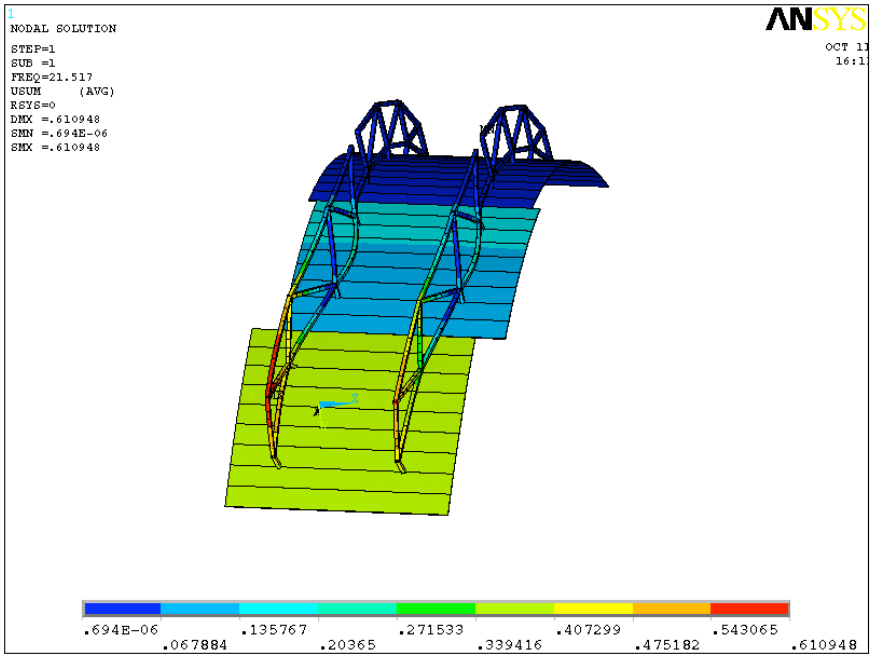

Figure 42 Orientation 210°, self-weight and wind 30m/s. First structural buckling mode, multiplying factor 21.5

It is necessary a load 21.5 higher than the one applied to cause the instability of the truss in this load condition, the structure appear therefore to be fairly safe.
The same model has also been analyzed under the action of the 15m/s wind in the 0° orientation. The first instability mode of the structure is shown in the following figure.

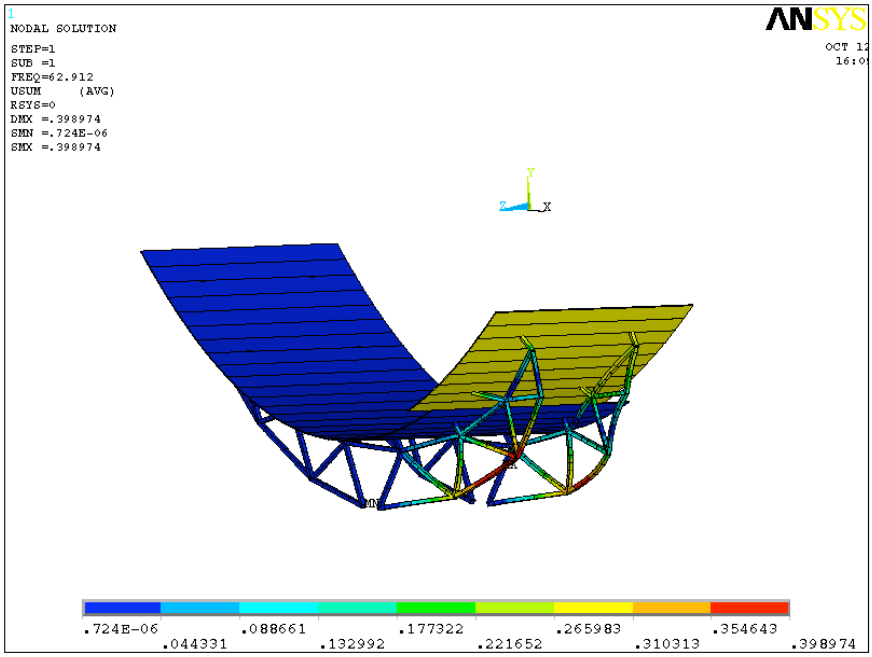

Figure 43 Orientation 0°, self-weight and wind 15m/s. First structural buckling mode, multiplying factor 62.9

The multiplying factor of the load is higher than 60, this means that the truss appears fairly safe with respect to buckling in this load condition: the truss structure would fail due to the material strength rather than be subject to an elastic instability.

Alternative design

The use of close shaped section has the drawback of causing some difficulties on the machining of the arms, and in particular for the drilling of the pass trough holes at the ends of the beams that are assembled to form the arms. A much easier assembling of the truss can be realized if open sections are adopted for the arms.
An alternative design has therefore been analyzed that adopts an L section with equal side length of 30mm and a thickness of 4mm. The thickness of the section has been doubled, in order to have the same weight and tensile strength of the close section of the original design.
But the open sections have a lower lateral stability than a close section with the same specific weight; it is therefore necessary to verify the structural stability of the two constructions with a detailed finite element model. In these models the truss is not modeled with beam/truss elements, but with shell elements, as can be seen in the detail pictures of the models shown hereafter.

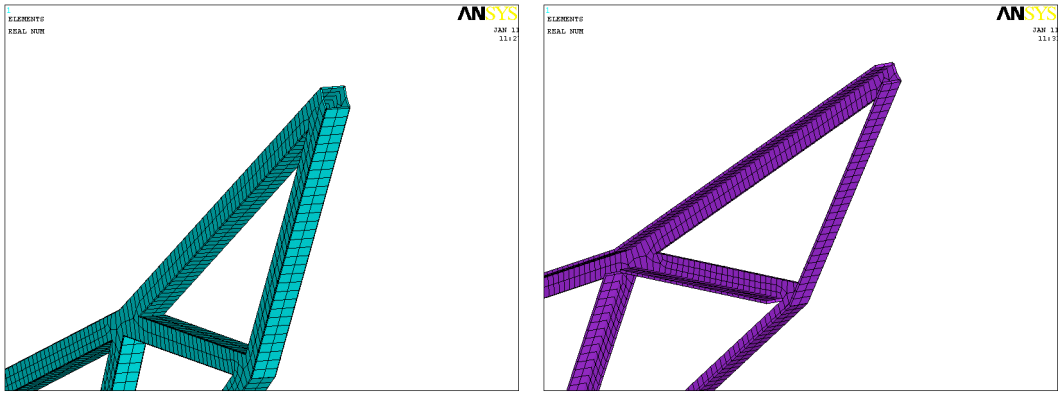

Figure 44 Finite element models of the close section arms (left) and of the open section arms (right).

A pair of arms has been analyzed, the connections to the structural tube are considered fixed and a vertical force of 100N has been applied to each of the mirror support points. This load is roughly equivalent to a pressure of 80Pa on each mirror.
The mirror stiffening effect was simulated adding rigid links between the arm-mirror support points.
The buckling analysis showed that the stiffness of the two designs is different: there is a factor of ten on the buckling strength of the closed section beams with respect to the open sections.
The following picture shows the first buckling mode resulting from the analysis of the close section arms; the load amplification factor is 100 on the load applied, the other buckling modes have higher amplification factors but are similar in the resulting deformation.

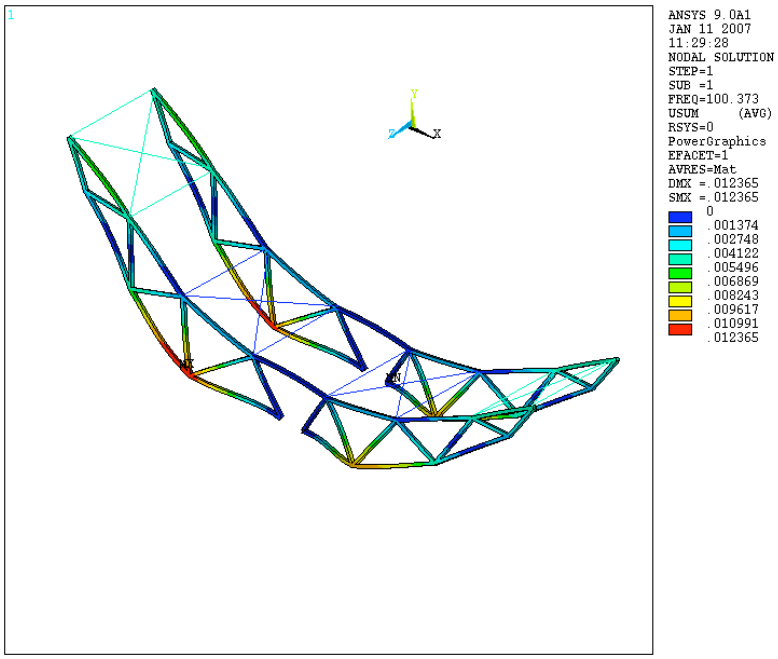

Figure 45 First buckling mode of the close section model: load amplification factor 100

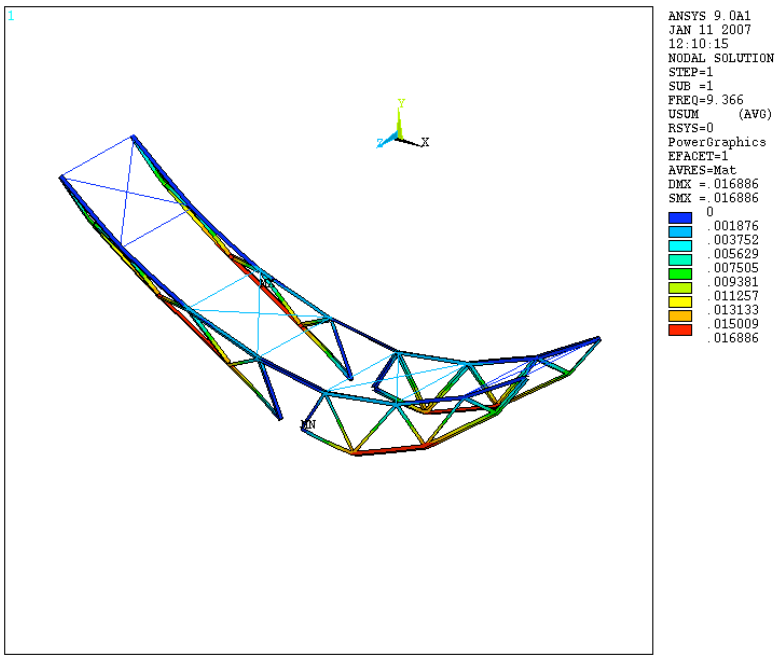

Figure 46 First buckling mode for the open section arms: load amplification factor 9.4

The analysis of the open section arms gave similar deformation modes, the first is shown in the picture above, but the corresponding load factor are ten times lower: 9.4 is the factor for the first mode.
The results show that the buckling stability of an open section design would be ten times lower than the close section design. Therefore the safety factors on buckling of the previous analyses would be much reduced adopting this alternate design. A factor 2 instead of 21 would result for the high wind condition; that appears not to be sufficient because of the damage that could be caused and of the approximation of the analyses.

Mirror analysis

A detailed mode of a mirror has been analyzed to verify its resistance under the heavier loading conditions. The loading condition has the mirror in protection condition, forming an angle of 210°, facing a wind of 30m/s with its back (non reflective) side. The gravity is considered as well. These loads caused the highest stresses on the mirror in the complete model previously discussed.
The results of the previous analyses have shown that the highest equivalent stresses where acting on the support points of the mirror, where the detail of the mesh was clearly not sufficient to consider these results to be affordable.
This is the reason for this more detailed model, in which the mirror supports are modeled with care.
The mirror has the parabolic shape already described, it has a width of approximately 1600mm and a length of 1740mm; it is supported in four points by cylindrical shaped supports, made by some plastic material, such as PVC, having a diameter of 10cm and a thickness of 2 cm, approximately.
The following figure shows the stress intensity resulting in the model with the mentioned load conditions.

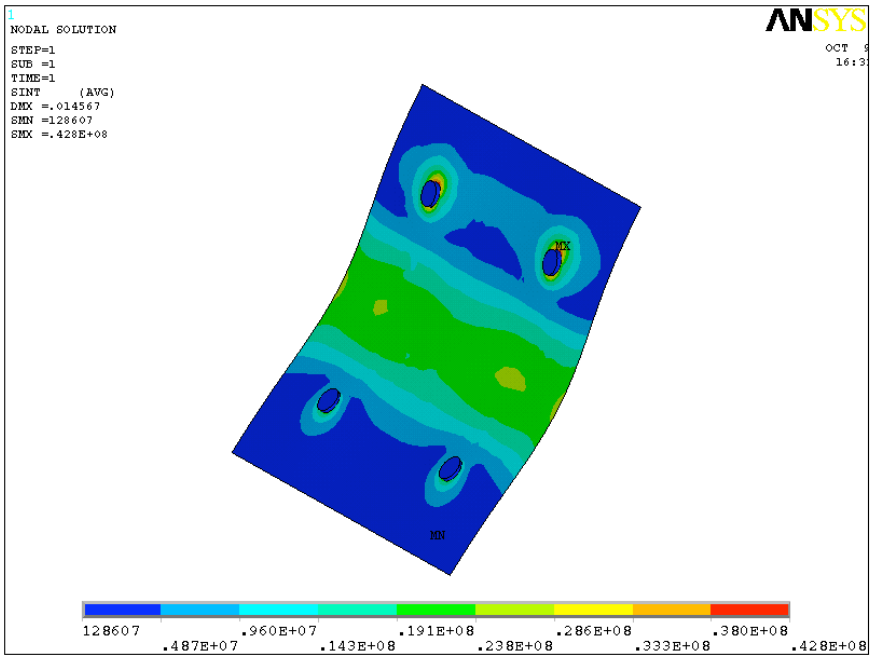

Figure 47 Orientation 210°, self-weight and wind 30m/s. Equivalent stress intensity in the mirror detailed model [Pa] (the displacements are magnified)

A stress concentration is still present near the supports, and the maximum Guest equivalent stress results in 43MPa. The stresses in the central part of the mirror surface result to be high as well, reaching 24MPa. The values found with this model are comparable, and only slightly lower than those found with the complete trough model, thus confirming the previous results.
Some kind of glass may reach a rupture stress value as high as 60MPa, under laboratory conditions. The aging of the material and of its surface greatly reduce the strength of the

material. The UNI code in fact fixes an allowable stress limit of 12MPa. The resulting stresses are therefore well beyond this limit.
When the wind reaches values as high as 30m/s some rupture have to be expected in the first trough line, and in the most external row of mirrors. In order to improve the strength of these mirrors and stay within the limits of the UNI code, the thickness should be increased to approximately 8mm!

Trough efficiency

It is now interesting to estimate the efficiency of the trough line under these loading conditions, and for other wind velocities.
To do this the results of the deformations of the mirrors of the 1st and 2nd module of a line (two modules per side, four modules per actuator) have been extracted by the finite element results, and the position of the reflected beam on the absorber tube has been calculated for each mirror element.
The most important movement of the mirror points is their rotation around an axis parallel to the absorber tube, since this can cause the reflected beam to fall out of focus and out of the absorber tube surface, that portion of the mirror surface would therefore lose its functions and mirror efficiency decrease.
Looking at the following figure we could easily see that the deviation of the beam on the tube surface (v) as an effect of the mirror rotation (α) may be calculated as:

$$v = 2r(\alpha)$$

With α is expressed in radians.

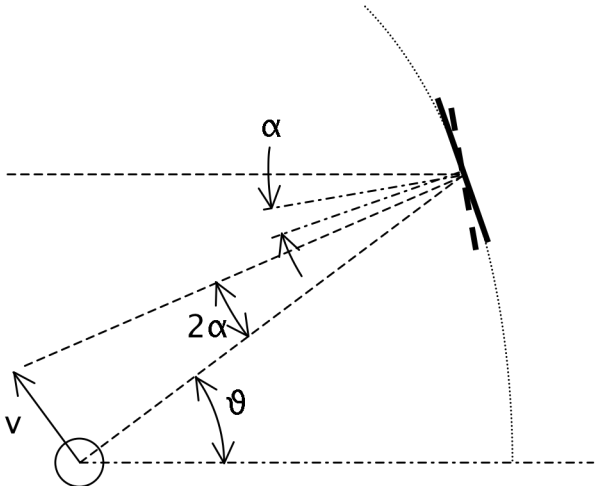

Figure 48 Beam position as an effect of mirror rotation

When the beam displacement is higher than the absorber tube radius, that portion of the mirror surface is not contributing to the energy balance.
If S is the mirror surface the power reflected to the absorber tube is calculated as follows:

$$W_{tube} = \int_S w_{sun} \cos(2\vartheta) f(\alpha) dS$$

where w_{sun} is the power form the sun per unit surface, cos(2ϑ) is the projection factor, and f is a function to evaluate if the portion of the surface is reflecting on the tube or not.

$$f(\alpha) = \begin{cases} 1 & 4r|\alpha| \le d \\ 0 & 4r|\alpha| > d \end{cases}$$

We have to consider that an error on the angle of the reflective surface may be also due to the constructive tolerances and to the errors in the pointing device and actuation system; we may identify with β this angle, and the function f becomes:

$$f(\alpha) = \begin{cases} 1 & 4r(|\alpha| + \beta) \le d \\ 0 & 4r(|\alpha| + \beta) > d \end{cases}$$

We analyzed the line with two modules, checking the efficiency of the line at different wind speeds. The efficiency is calculated as the ratio between the reflected sun power that reaches the absorber tube with the maximum theoretical reflected power that reaches the tube, in case no deformation occurs.
In the following graph we suppose that the angle β of the tolerance is equal to 4mrad, and we show the line efficiency ad different wind speed for an orientation of 0°.

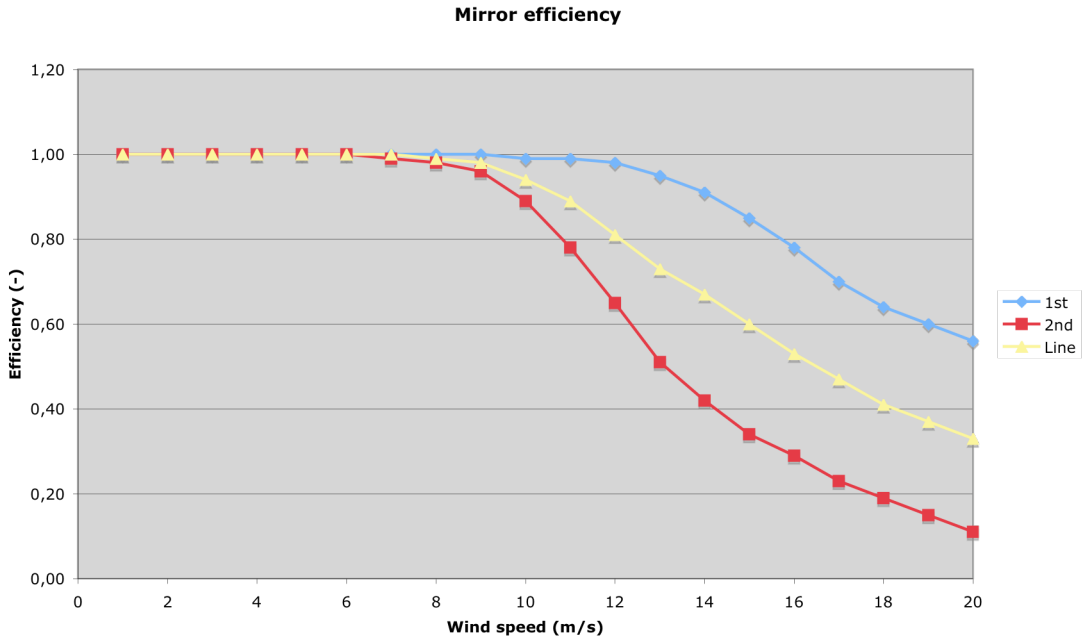

Figure 49 Mirror efficiency due to the deformation under wind and gravity load

It is possible to verify from the graph that the line does not suffer winds up to 7m/s. With higher winds the 2nd module has worse performances and after 12m/s also the 1st module; at 15m/s the line has an efficiency due to the errors and deformation of the reflective surface of 60%.
Of course in case the constructive tolerances are lower and the actuation system is stiffer and more precise, it would be possible to have a lower estimation of β and better overall results.

Vibration analysis

A modal analysis was run on the trough model to look after the vibration modes of the structure, and their frequencies.
Two trough lines are considered, in the first example the line s formed by two modules, one for each side of the actuator and the total length of the line is approximately 25m; in the second case the line is 50m long, is formed by 4 modules, two for each side of the actuator.
Looking at the “short” line, the model adopted is the same previously described of a single trough module. Looking for the vibration modes with the lower frequencies, both bending and torsion modes are found, as expected.
The bending modes are orthogonal one to the other, the lateral bending has a frequency of 3.53Hz and vertical bending mode has a similar frequency of 3.76Hz, the higher value is due to the (moderate) stiffening effect of the cantilever arms for this deformation.
Then the first torsion mode was found at a frequency of 4.53Hz.
The following modes involve movements of the mirrors and of the cantilever arms; there are lots of similar vibration modes, with similar frequency. These vibration modes do not appear to be important for the structural safety since the loads acting on the trough can hardly force these movements.

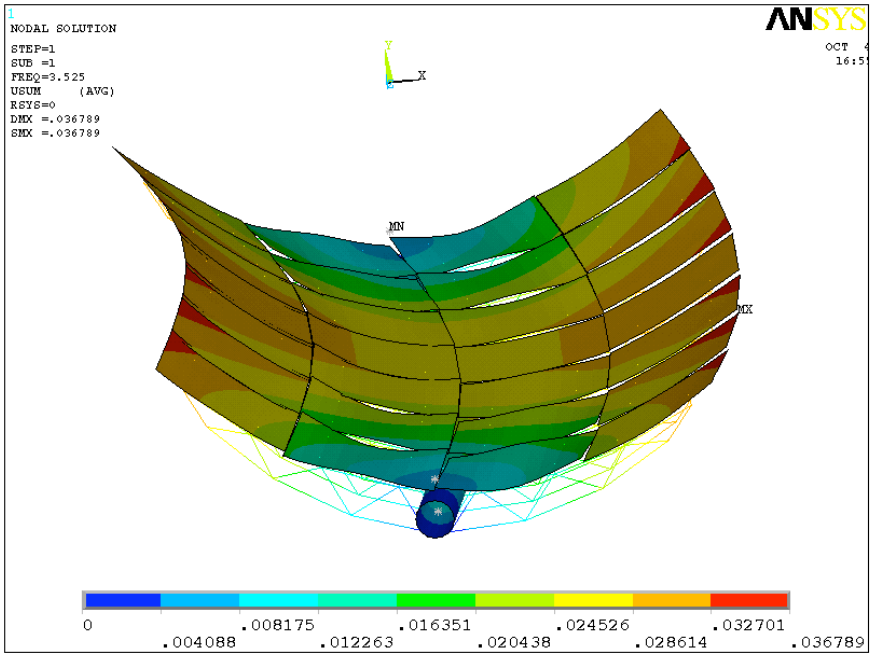

Figure 50 Horizontal bending mode of the through module, f=3.53Hz.

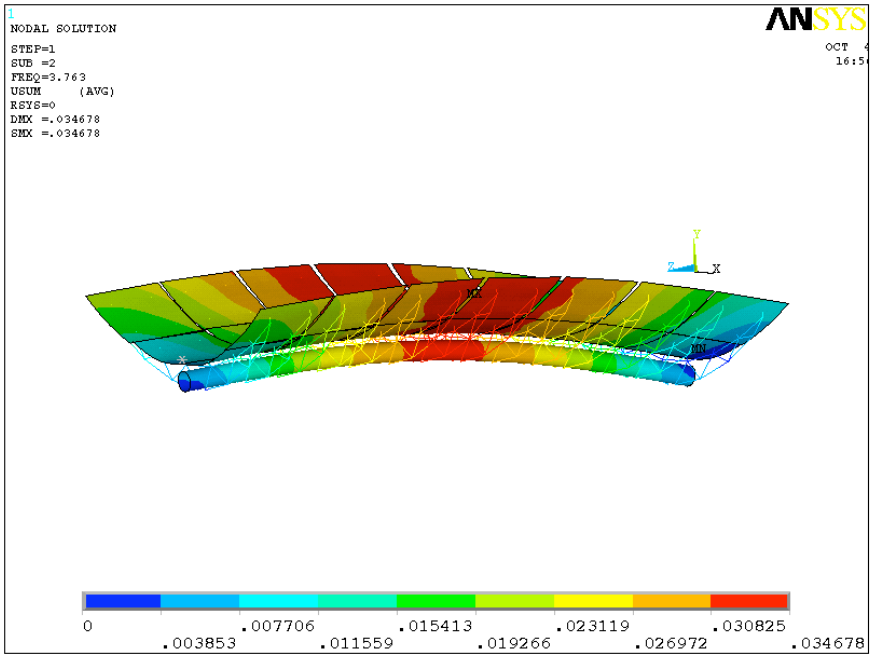

Figure 51 Vertical bending mode of the through module, f=3.76Hz

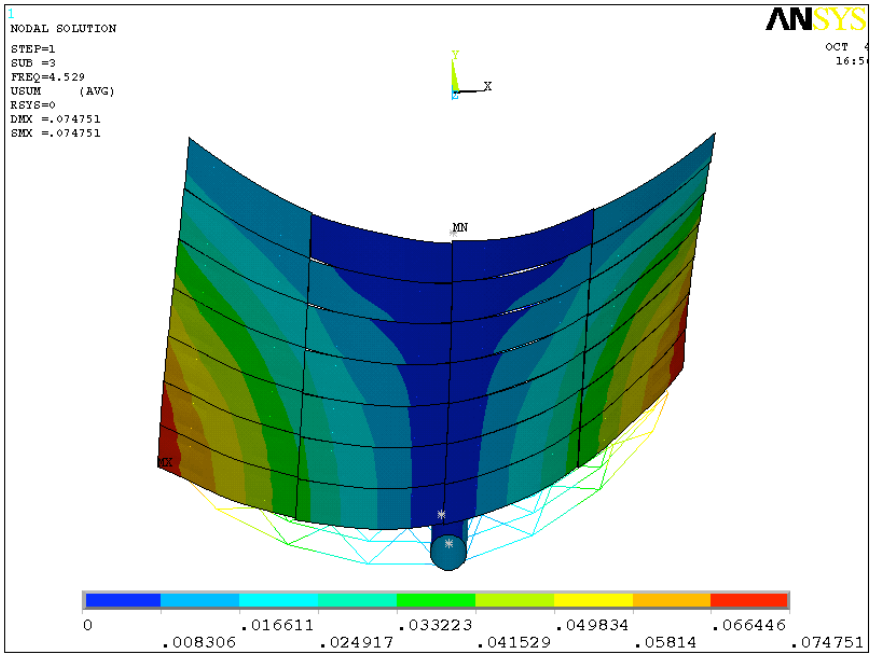

Figure 52 Torsion mode of the through module, f=4.53Hz

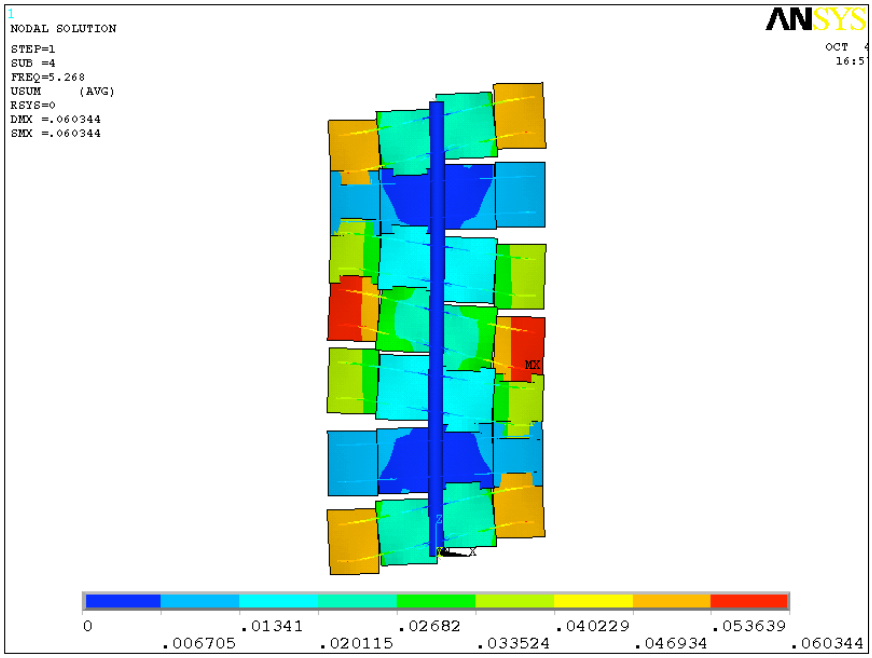

Figure 53 Inutil mode of the through module, f=5.27Hz

Two trough modules linked form a “long” line. The rotation around the axis is the same but the two trough modules may be considered independent for bending. As a result the bending vibration modes are the same found for the single trough shown previously, and the frequency is the same. The differences are in the torsion of the line, with a lower frequency (2.30Hz) torsion mode appearing; the second torsion mode is similar and has the same frequency of the first model of the “short” line.

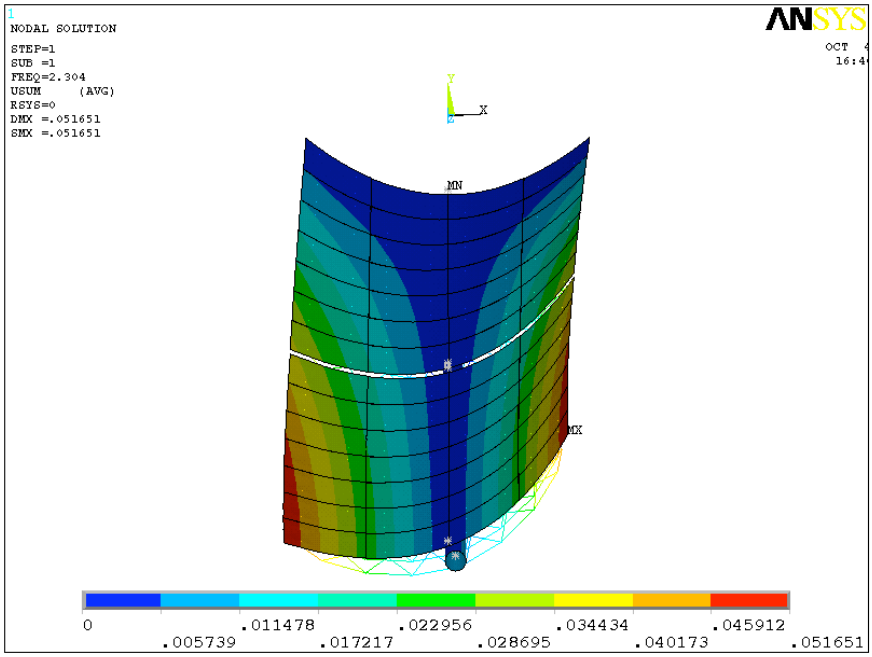

Figure 54 Torsion mode of the through line, f=2.30Hz

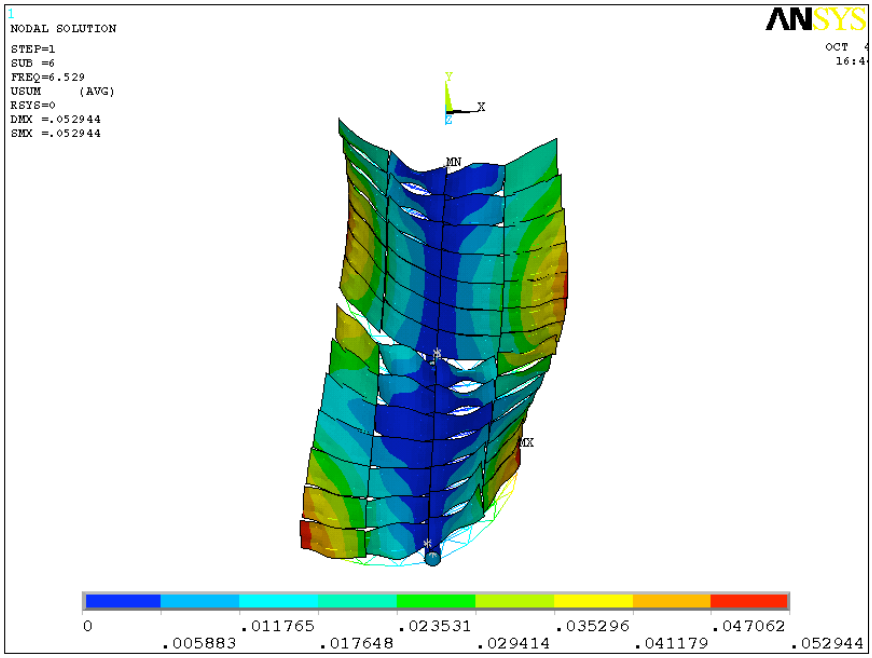

Figure 55 Torsion mode of the through line, f=4.53Hz

The modal analysis shows the vibration modes and their frequencies. These vibrations may be dangerous or not depending only on the loads acting on it.
The higher frequency modes involving the bending of the cantilever arms and the mirror movement along the axis, does not appear to be important since is hard to figure out how this vibration may be harmonically excited.
On the other side the bending vibrations may be harmonically excited by the action of the wind loads and the interaction between the deformations of the structure and the aerodynamics. A dedicated CFD analysis may be required.
Torsion mode appear to be interesting as well, since these vibration may be harmonically forced by the aerodynamics, and also by the action of the actuating system.

In particular the vibration frequencies should be of interest in the design of the actuator to avoid any resonance between the line vibration and the actuator.

Conclusions

The structure of the trough module has been analyzed by means of Finite Element Analyses. Investigating on the deformations, strength and rigidity of the structure.
The load conditions applied are representative of an operating condition, when the sun is at the azimuth, and a lateral wind is blowing at 15m/s; and of the emergency condition when a wind of 30m/s is blowing and the trough line is put in protection position.
The strength of the structure according to the model appear to be sufficient in the load conditions examined, with the exception of the mirrors that have an high probability of rupture when high winds are acting on the structure. The first line of the mirrors of the first line of the trough may need to be reinforced, adopting a thicker glass for instance, unless some rupture of the mirrors may be tolerated during the operative lifetime. Another option to avoid these problems would be adopting some means to reduce the wind pressure on the mirrors (with a line of trees for instance).
In the following table the maximum stresses found on the structure and mirrors and the loads on the supports are shown, for the load cases examined.

Table 3 Results for load case 1: Gravity load, orientation 0°

Maximum stress on mirrors	4.8	MPa
Maximum stress on arms	7.3	MPa
Maximum stress on tube	58.6	MPa
Maximum deflection	21.9	mm
Maximum mirror rotation	2.3	mrad
Vertical force on the support	17820	N
Transverse force on the support	0	N
Actuator torque	0	Nm

Table 4 Results for load case 1: Gravity load, orientation 30°, and 210°

Maximum stress on mirrors	5.6	MPa
Maximum stress on arms	8.1	MPa
Maximum stress on tube	58.1	MPa
Maximum deflection	22.9	mm
Maximum mirror rotation	3.1	mrad
Vertical force on the support	17820	N
Transverse force on the support	0	N
Actuator torque	612	Nm

Table 5 Results for load case 1: Gravity load, wind at 30m/s, orientation 210°

Maximum stress on mirrors	40	MPa
Maximum stress on arms	33.8	MPa
Maximum stress on tube	62.5	MPa
Maximum deflection	-	mm
Maximum mirror rotation	-	mrad
Vertical force on the support	14216	N
Transverse force on the support	15016	N
Actuator torque	0	Nm

Table 6 Results for load case 1: Gravity load, wind 15m/s, orientation 0°, 50m long line

Maximum stress on mirrors	6.9	MPa
Maximum stress on arms	10.7	MPa
Maximum stress on tube	58.5	MPa
Maximum deflection	37.8	mm
Maximum mirror rotation	10.8	mrad

Vertical force on the support	17648	N
Transverse force on the support	624	N
Actuator torque	10956	Nm

The structure has been also analyzed with respect to structural buckling, and the model showed satisfactory results.
The mirror deformation results in the operative conditions have been used to calculate the mirror efficiency in reflecting the solar power towards the target absorber tube.
It results that this efficiency depends mainly by the torsion stiffness of the structural tube and by the length of the trough line, and also by the bending stiffness of the mirrors.
The line considered has a total length of 50m, it is formed by four modules, two per actuator side. In this condition and including the tolerances in the construction and assembly of the structure, it results that the reflecting efficiency decreases for wind velocities higher than 7m/s, a value generally considered as a practical limit. In order to keep higher mirror efficiencies for high wind speed, a stiffer structural tube should be adopted, either increasing the thickness, or (better) increasing the diameter.
The structure seems to have a satisfactory behavior for the analyses run so far. It would be anyway be preferable to examine other operative conditions to verify the strength and stiffness of the structure and to determine the actuator torque required.